

# Applications of Mathematics

---

Larisa Beilina; Samar Hosseinzadegan

An adaptive finite element method in reconstruction of coefficients in Maxwell's equations from limited observations

*Applications of Mathematics*, Vol. 61 (2016), No. 3, 253–286

Persistent URL: <http://dml.cz/dmlcz/145701>

## Terms of use:

© Institute of Mathematics AS CR, 2016

Institute of Mathematics of the Czech Academy of Sciences provides access to digitized documents strictly for personal use. Each copy of any part of this document must contain these *Terms of use*.



This document has been digitized, optimized for electronic delivery and stamped with digital signature within the project *DML-CZ: The Czech Digital Mathematics Library* <http://dml.cz>

AN ADAPTIVE FINITE ELEMENT METHOD  
IN RECONSTRUCTION OF COEFFICIENTS  
IN MAXWELL'S EQUATIONS FROM LIMITED OBSERVATIONS

LARISA BEILINA, SAMAR HOSSEINZADEGAN, Göteborg

(Received December 4, 2015)

*Abstract.* We propose an adaptive finite element method for the solution of a coefficient inverse problem of simultaneous reconstruction of the dielectric permittivity and magnetic permeability functions in the Maxwell's system using limited boundary observations of the electric field in 3D.

We derive a posteriori error estimates in the Tikhonov functional to be minimized and in the regularized solution of this functional, as well as formulate the corresponding adaptive algorithm. Our numerical experiments justify the efficiency of our a posteriori estimates and show significant improvement of the reconstructions obtained on locally adaptively refined meshes.

*Keywords:* Maxwell's system; coefficient inverse problem; Tikhonov functional; Lagrangian approach; a posteriori error estimate

*MSC 2010:* 65M06, 65N30, 65M60, 65M22, 65M32

## 1. INTRODUCTION

This work is a continuation of the recent paper [6] and is focused on the numerical reconstruction of the dielectric permittivity  $\varepsilon(x)$  and the magnetic permeability  $\mu(x)$  functions in Maxwell's system on locally refined meshes using an adaptive finite element method. The reconstruction is performed via minimization of the corresponding Tikhonov functional from backscattered single measurement data of the electric field  $E(x, t)$ . That means that we use backscattered boundary measurements of the wave field  $E(x, t)$  which are generated by a single direction of a plane wave. In the

---

This research is supported by the Swedish Research Council (VR). The computations were performed on resources at Chalmers Centre for Computational Science and Engineering (C3SE) provided by the Swedish National Infrastructure for Computing (SNIC).

minimization procedure we use domain decomposition finite element/finite difference methods of [5] for the numerical reconstructions of both the functions.

Comparing with [6], we present the following new points here: we adopt results of [8], [9], [21] to show that the minimizer of the Tikhonov functional is closer to the exact solution than a guess of this solution. We present the relaxation property for the mesh refinements for the case of our inverse problem and derive a posteriori error estimates for the error in the minimization functional and in the reconstructed functions  $\varepsilon(x)$  and  $\mu(x)$ . Further, we formulate two adaptive algorithms and apply them in the reconstruction of small inclusions. Moreover, in our numerical simulations of this work we induce inhomogeneous initial conditions in Maxwell's system. Non-zero initial conditions involve uniqueness and stability results of reconstruction of both the unknown functions  $\varepsilon(x)$  and  $\mu(x)$ , see details in [6], [11]. Using our numerical simulations we can conclude that an adaptive finite element method can significantly improve reconstructions obtained on a coarse non-refined mesh in order to accurately obtain shapes, locations and values of functions  $\varepsilon(x)$  and  $\mu(x)$ .

An outline of this paper is as follows: in Section 2 we present our mathematical model and in Section 3 we formulate forward and inverse problems. In Section 4 we present the Tikhonov functional to be minimized and in Section 5 we show different versions of the finite element method used in computations. In Section 6 we formulate the relaxation property of mesh refinements and in Section 7 we investigate the general framework of a posteriori error estimates in coefficient inverse problems (CIPs). In Sections 8, 9 we present theorems for a posteriori errors in the regularized solution of the Tikhonov functional and in the Tikhonov functional, correspondingly. In Sections 10, 11 we describe mesh refinement recommendations and formulate adaptive algorithms used in computations. Finally, in Section 12 we present our reconstruction results.

## 2. THE MATHEMATICAL MODEL

Let a bounded domain  $\Omega \subset \mathbb{R}^d$ ,  $d = 2, 3$ , have Lipschitz boundary  $\partial\Omega$  and let us set  $\Omega_T := \Omega \times (0, T)$ ,  $\partial\Omega_T := \partial\Omega \times (0, T)$ , where  $T > 0$ . We consider Maxwell's equations in an inhomogeneous isotropic media in a bounded domain  $\Omega \subset \mathbb{R}^3$

$$(2.1) \quad \begin{cases} \partial_t D - \nabla \times H(x, t) = 0 & \text{in } \Omega_T \\ \partial_t B + \nabla \times E(x, t) = 0 & \text{in } \Omega_T, \\ D(x, t) = \varepsilon E(x, t), \quad B(x, t) = \mu H(x, t), \\ E(x, 0) = E_0(x), \quad H(x, 0) = H_0(x), \\ \nabla \cdot D(x, t) = 0, \quad \nabla \cdot B(x, t) = 0 & \text{in } \Omega_T, \\ n \times D(x, t) = 0, \quad n \cdot B(x, t) = 0 & \text{on } \partial\Omega_T, \end{cases}$$

where  $x = (x_1, x_2, x_3)$ . Here,  $E(x, t)$  is the electric field and  $H(x, t)$  is the magnetic field,  $\varepsilon(x) > 0$  and  $\mu(x) > 0$  are the dielectric permittivity and the magnetic permeability functions, respectively,  $E_0(x)$  and  $H_0(x)$  are given initial conditions. Next,  $n = n(x)$  is the unit outward normal vector to  $\partial\Omega$ . The electric field  $E(x, t)$  is combined with the electric induction  $D(x, t)$  via

$$D(x, t) = \varepsilon E(x, t) = \varepsilon_{\text{vac}} \varepsilon_r E(x, t),$$

where  $\varepsilon_{\text{vac}} \approx 8.854 \times 10^{-12}$  is the vacuum permittivity which is measured in Farads per meter, and thus  $\varepsilon_r$  is the dimensionless relative permittivity. The magnetic field  $H(x, t)$  is combined with the magnetic induction  $B(x, t)$  via

$$B(x, t) = \mu H(x, t) = \mu_{\text{vac}} \mu_r H(x, t),$$

where  $\mu_{\text{vac}} \approx 1.257 \times 10^{-6}$  is the vacuum permeability measured in Henries per meter, which implies that  $\mu_r$  is the dimensionless relative permeability.

By eliminating  $B$  and  $D$  from (2.1), we obtain the model problem for the electric field  $E$  with the perfectly conducting boundary conditions:

$$(2.2) \quad \varepsilon \frac{\partial^2 E}{\partial t^2} + \nabla \times (\mu^{-1} \nabla \times E) = 0 \quad \text{in } \Omega_T,$$

$$(2.3) \quad \nabla \cdot (\varepsilon E) = 0 \quad \text{in } \Omega_T,$$

$$(2.4) \quad E(x, 0) = f_0(x), \quad E_t(x, 0) = f_1(x) \quad \text{in } \Omega,$$

$$(2.5) \quad E \times n = 0 \quad \text{on } \partial\Omega_T.$$

Here we assume that

$$f_0 \in H^1(\Omega), f_1 \in L^2(\Omega).$$

By this notation we shall mean that every component of the vector functions  $f_0$  and  $f_1$  belongs to these spaces. Note that equations similar to (2.2)–(2.5) can be derived also for the magnetic field  $H$ .

As in our recent work [6], for the discretization of Maxwell's equations we use a stabilized domain decomposition method of [4]. In our numerical simulations we assume that the relative permittivity  $\varepsilon_r$  and relative permeability  $\mu_r$  do not vary much, which is the case of real applications, see recent experimental work [10] for similar observations. We do not impose smoothness assumptions on the coefficients  $\varepsilon(x)$ ,  $\mu(x)$  and we treat discontinuities in a way similar to [13]. Thus, a discontinuous finite element method should be applied for the finite element discretization of these functions, see details in Section 5.

### 3. STATEMENTS OF FORWARD AND INVERSE PROBLEMS

We divide  $\Omega$  into two subregions,  $\Omega_{\text{FEM}}$  and  $\Omega_{\text{OUT}}$  such that  $\overline{\Omega} = \overline{\Omega_{\text{FEM}}} \cup \overline{\Omega_{\text{OUT}}}$ ,  $\Omega_{\text{FEM}} \cap \Omega_{\text{OUT}} = \emptyset$ , and  $\partial\Omega_{\text{FEM}} \subset \partial\Omega_{\text{OUT}}$ . For an illustration of the domain decomposition, see Figure 1. The boundary  $\partial\Omega$  is such that  $\partial\Omega = \partial_1\Omega \cup \partial_2\Omega \cup \partial_3\Omega$ , where  $\partial_1\Omega$  and  $\partial_2\Omega$  are, respectively, front and back sides of the domain  $\Omega$ , and  $\partial_3\Omega$  is the union of left, right, top and bottom faces of this domain. For numerical solution of (2.2)–(2.5) in  $\Omega_{\text{OUT}}$  we can use either the finite difference or the finite element method on a structured mesh with constant coefficients  $\varepsilon = 1$  and  $\mu = 1$ . In  $\Omega_{\text{FEM}}$ , we use finite elements on a sequence of unstructured meshes  $K_h = \{K\}$ , with elements  $K$  consisting of triangles in  $\mathbb{R}^2$  and tetrahedra in  $\mathbb{R}^3$  satisfying the maximal angle condition [12].

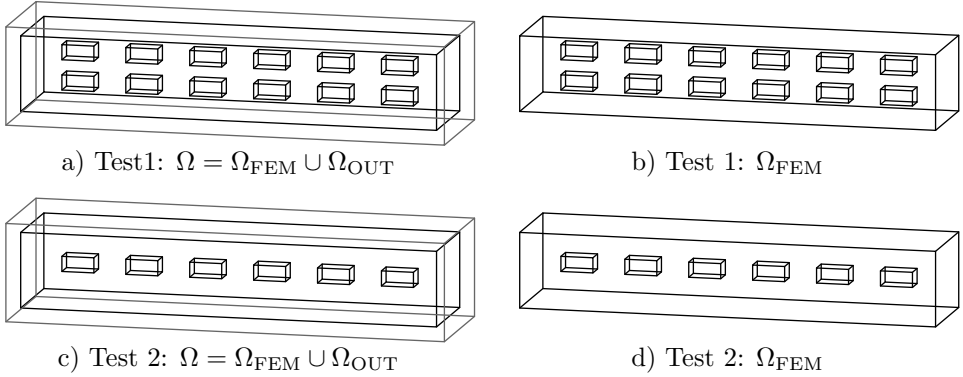


Figure 1. Domain decomposition in numerical tests of Section 12. a), c) The decomposed domain  $\Omega = \Omega_{\text{FEM}} \cup \Omega_{\text{OUT}}$ . b), d) The finite element domain  $\Omega_{\text{FEM}}$ .

Let  $S_T := \partial_1\Omega \times (0, T)$ , where  $\partial_1\Omega$  is the backscattering side of the domain  $\Omega$  with the time domain observations, and define  $S_{1,1} := \partial_1\Omega \times (0, t_1]$ ,  $S_{1,2} := \partial_1\Omega \times (t_1, T)$ ,  $S_2 := \partial_2\Omega \times (0, T)$ ,  $S_3 := \partial_3\Omega \times (0, T)$ .

To simplify notation, further we will omit subscript  $r$  in  $\varepsilon_r$  and  $\mu_r$ . We add a Coulomb-type gauge condition [1], [26] to (2.2)–(2.5) for stabilization of the finite element solution using the standard piecewise continuous functions with  $0 \leq s \leq 1$ , and our model problem (2.2)–(2.5) which we use in computations rewrites as

$$\begin{aligned}
 (3.1) \quad & \varepsilon \frac{\partial^2 E}{\partial t^2} + \nabla \times (\mu^{-1} \nabla \times E) - s \nabla (\nabla \cdot (\varepsilon E)) = 0 \quad \text{in } \Omega_T, \\
 & E(x, 0) = f_0(x), \quad E_t(x, 0) = f_1(x) \quad \text{in } \Omega, \\
 & \partial_n E = (0, f(t), 0) \quad \text{on } S_{1,1}, \quad \partial_n E = -\partial_t E \quad \text{on } S_{1,2}, \\
 & \partial_n E = -\partial_t E \quad \text{on } S_2, \quad \partial_n E = 0 \quad \text{on } S_3, \\
 & \mu(x) = \varepsilon(x) = 1 \quad \text{in } \Omega_{\text{OUT}}.
 \end{aligned}$$

In the recent works [5], [6], [10] it was demonstrated numerically that the solution of the problem (3.1) approximates well the solution of the original Maxwell's system for the case when  $1 \leq \mu(x) \leq 2$ ,  $1 \leq \varepsilon(x) \leq 15$  and  $s = 1$ .

We assume that our coefficients  $\varepsilon(x)$ ,  $\mu(x)$  of equation (3.1) are such that

$$(3.2) \quad \begin{aligned} \varepsilon(x) &\in [1, d_1], \quad d_1 = \text{const.} > 1, \quad \varepsilon(x) = 1 \text{ for } x \in \Omega_{\text{OUT}}, \\ \mu(x) &\in [1, d_2], \quad d_2 = \text{const.} > 1, \quad \mu(x) = 1 \text{ for } x \in \Omega_{\text{OUT}}. \end{aligned}$$

In our numerical tests the values of constants  $d_1, d_2$  in (3.2) are chosen from experimental set-up similarly to [10], [30] and we assume that we know them a priori.

This is in agreement with the availability of a priori information for an ill-posed problem [2], [16], [32]. Through the work we use the following notation: for any vector function  $u \in \mathbb{R}^3$  when we write  $u \in H^k(\Omega)$ ,  $k = 1, 2$ , we mean that every component of the vector function  $u$  belongs to this space. We consider the following

**Inverse Problem (IP).** Assume that the functions  $\varepsilon(x)$  and  $\mu(x)$  satisfy conditions (3.2) for the known  $d_1, d_2 > 1$  and are unknown in the domain  $\Omega \setminus \Omega_{\text{OUT}}$ . Determine the functions  $\varepsilon(x), \mu(x)$  for  $x \in \Omega \setminus \Omega_{\text{OUT}}$ , assuming that the following function  $\tilde{E}(x, t)$  is known:

$$(3.3) \quad E(x, t) = \tilde{E}(x, t) \quad \forall (x, t) \in S_T.$$

The function  $\tilde{E}(x, t)$  in (3.3) represents the time-dependent measurements of the electric wave field  $E(x, t)$  on the backscattering boundary  $\partial_1\Omega$ . In real-life experiments, measurements are performed on a number of detectors, see details in our recent experimental work [10].

#### 4. TIKHONOV FUNCTIONAL

We reformulate our inverse problem as an optimization problem, where we seek for two functions, the permittivity  $\varepsilon(x)$  and permeability  $\mu(x)$ , which result in a solution of equations (3.1) with best fit to time and space domain observations  $\tilde{E}$ , measured at a finite number of observation points on  $\partial_1\Omega$ . Our goal is to minimize the Tikhonov functional

$$(4.1) \quad \begin{aligned} J(\varepsilon, \mu) := J(E, \varepsilon, \mu) &= \frac{1}{2} \int_{S_T} (E - \tilde{E})^2 z_\delta(t) \, d\sigma \, dt \\ &+ \frac{1}{2} \gamma_1 \int_{\Omega} (\varepsilon - \varepsilon_0)^2 \, dx + \frac{1}{2} \gamma_2 \int_{\Omega} (\mu - \mu_0)^2 \, dx, \end{aligned}$$

where  $\tilde{E}$  is the observed electric field,  $E$  satisfies the equations (3.1) and thus depends on  $\varepsilon$  and  $\mu$ ,  $\varepsilon_0$  is the initial guess for  $\varepsilon$  and  $\mu_0$  is the initial guess for  $\mu$ , and  $\gamma_i$ ,  $i = 1, 2$ , are the regularization parameters. Here,  $z_\delta(t)$  is a cut-off function, which is introduced to ensure that the compatibility conditions at  $\bar{\Omega}_T \cap \{t = T\}$  for the adjoint problem (4.10) are satisfied, and  $\delta > 0$  is a small number. The function  $z_\delta$  can be chosen as in [6].

Next, we introduce the spaces of real valued vector functions

$$(4.2) \quad \begin{aligned} H_E^1 &:= \{w \in H^1(\Omega_T) : w(\cdot, 0) = 0\}, \\ H_\lambda^1 &:= \{w \in H^1(\Omega_T) : w(\cdot, T) = 0\}, \\ U^1 &= H_E^1(\Omega_T) \times H_\lambda^1(\Omega_T) \times C(\bar{\Omega}) \times C(\bar{\Omega}), \\ U^0 &= L^2(\Omega_T) \times L^2(\Omega_T) \times L^2(\Omega) \times L^2(\Omega). \end{aligned}$$

We also define the  $L^2$  inner product and the norm over  $\Omega_T$  and  $\Omega$  as

$$\begin{aligned} ((u, v))_{\Omega_T} &= \int_{\Omega} \int_0^T uv \, dx \, dt, \\ \|u\|^2 &= ((u, u))_{\Omega_T}, \\ (u, v)_{\Omega} &= \int_{\Omega} uv \, dx, \\ |u|^2 &= (u, u)_{\Omega}. \end{aligned}$$

To solve the minimization problem we take into account (3.2) and introduce the Lagrangian

$$(4.3) \quad \begin{aligned} L(u) &= J(E, \varepsilon, \mu) - ((\varepsilon \partial_t \lambda, \partial_t E))_{\Omega_T} - (\varepsilon \lambda(x, 0), f_1(x))_{\Omega} + ((\mu^{-1} \nabla \times E, \nabla \times \lambda))_{\Omega_T} \\ &\quad + s((\nabla \cdot (\varepsilon E), \nabla \cdot \lambda))_{\Omega_T} - ((\lambda, p(t)))_{S_{1,1}} + ((\lambda \partial_t E))_{S_{1,2}} + ((\lambda \partial_t E))_{S_2}, \end{aligned}$$

where  $u = (E, \lambda, \varepsilon, \mu) \in U^1$  and  $p(t) = (0, f(t), 0)$ , and  $\partial_t$  define the derivative in time. We now search for a stationary point of the Lagrangian with respect to  $u$  satisfying for all  $\bar{u} = (\bar{E}, \bar{\lambda}, \bar{\varepsilon}, \bar{\mu}) \in U^1$

$$(4.4) \quad L'(u; \bar{u}) = 0,$$

where  $L'(u; \cdot)$  is the Jacobian of  $L$  at  $u$ . The equation above can be written as

$$(4.5) \quad L'(u; \bar{u}) = \frac{\partial L}{\partial \lambda}(u)(\bar{\lambda}) + \frac{\partial L}{\partial E}(u)(\bar{E}) + \frac{\partial L}{\partial \varepsilon}(u)(\bar{\varepsilon}) + \frac{\partial L}{\partial \mu}(u)(\bar{\mu}) = 0.$$

To find the Fréchet derivative (4.5) of the Lagrangian (4.3) we consider  $L(u + \bar{u}) - L(u)$  for all  $\bar{u} \in U^1$  and single out the linear part of the obtained expression with

respect to  $\bar{u}$ . In our derivation of the Fréchet derivative we assume that in the Lagrangian (4.3) the functions  $u = (E, \lambda, \varepsilon, \mu) \in U^1$  can vary independently of each other. In this approach we obtain the same result as by assuming that the functions  $E$  and  $\lambda$  are dependent on the coefficients  $\varepsilon, \mu$ , see also Chapter 4 of [8] where similar observations take place. Taking into account that  $E(x, t)$  is the solution of the forward problem (3.1), assumptions that  $\lambda(x, T) = (\partial\lambda/\partial t)(x, T) = 0$  as well as  $\mu = \varepsilon = 1$  on  $\partial\Omega$ , and using conditions (3.2), we obtain from (4.5) that for all  $\bar{u}$

$$(4.6) \quad 0 = \frac{\partial L}{\partial \lambda}(u)(\bar{\lambda}) = -((\varepsilon \partial_t \bar{\lambda}, \partial_t E)_{\Omega_T} - (\varepsilon f_1(x), \bar{\lambda}(x, 0))_{\Omega} + ((\mu^{-1} \nabla \times E, \nabla \times \bar{\lambda}))_{\Omega_T} + s((\nabla \cdot (\varepsilon E), \nabla \cdot \bar{\lambda}))_{\Omega_T} - ((\bar{\lambda}, p(t)))_{S_{1,1}} + ((\bar{\lambda}, \partial_t E)_{S_{1,2}} + ((\bar{\lambda}, \partial_t E)_{S_2} \quad \forall \bar{\lambda} \in H_{\lambda}^1(\Omega_T),$$

$$(4.7) \quad 0 = \frac{\partial L}{\partial E}(u)(\bar{E}) = ((E - \tilde{E}, \bar{E} z_{\delta})_{S_T} - ((\varepsilon \partial_t \lambda, \partial_t \bar{E}))_{\Omega_T} + ((\mu^{-1} \nabla \times \lambda, \nabla \times \bar{E}))_{\Omega_T} + s((\nabla \cdot \lambda, \nabla \cdot (\varepsilon \bar{E})))_{\Omega_T} - ((\partial_t \lambda, \bar{E}))_{S_{1,2} \cup S_2} - (\varepsilon \bar{E}(x, 0), \partial_t \lambda(x, 0)) \quad \forall \bar{E} \in H_E^1(\Omega_T).$$

Further, we obtain two equations that express that the gradients with respect to  $\varepsilon$  and  $\mu$  vanish:

$$(4.8) \quad 0 = \frac{\partial L}{\partial \varepsilon}(u)(\bar{\varepsilon}) = -((\partial_t \lambda, \partial_t E \bar{\varepsilon}))_{\Omega_T} - (\lambda(x, 0), f_1(x) \bar{\varepsilon})_{\Omega} + s((\nabla \cdot (\bar{\varepsilon} E), \nabla \cdot \lambda))_{\Omega_T} + \gamma_1(\varepsilon - \varepsilon_0, \bar{\varepsilon})_{\Omega} \quad \forall x \in \Omega,$$

$$(4.9) \quad 0 = \frac{\partial L}{\partial \mu}(u)(\bar{\mu}) = -((\mu^{-2} \nabla \times E, \nabla \times \lambda \bar{\mu}))_{\Omega_T} + \gamma_2(\mu - \mu_0, \bar{\mu})_{\Omega} \quad \forall x \in \Omega.$$

We observe that the equation (4.6) is the weak formulation of the state equation (3.1) and the equation (4.7) is the weak formulation of the adjoint problem

$$(4.10) \quad \varepsilon \frac{\partial^2 \lambda}{\partial t^2} + \nabla \times (\mu^{-1} \nabla \times \lambda) - s \varepsilon \nabla (\nabla \cdot \lambda) = -(E - \tilde{E})|_{S_T z_{\delta}} \quad \text{in } \Omega_T,$$

$$\lambda(\cdot, T) = \frac{\partial \lambda}{\partial t}(\cdot, T) = 0,$$

$$\partial_n \lambda = \partial_t \lambda \quad \text{on } S_{1,2},$$

$$\partial_n \lambda = \partial_t \lambda \quad \text{on } S_2,$$

$$\partial_n \lambda = 0 \quad \text{on } S_3,$$

which is solved backward in time.

We now define by  $E(\varepsilon, \mu), \lambda(\varepsilon, \mu)$  the exact solutions of the forward and adjoint problems for given  $\varepsilon, \mu$ , respectively. Then defining

$$u(\varepsilon, \mu) = (E(\varepsilon, \mu), \lambda(\varepsilon, \mu), \varepsilon, \mu) \in U^1,$$

using the fact that for exact solutions  $E(\varepsilon, \mu), \lambda(\varepsilon, \mu)$  because of (4.3), we have

$$(4.11) \quad J(E(\varepsilon, \mu), \varepsilon, \mu) = L(u(\varepsilon, \mu)).$$

Assuming that the solutions  $E(\varepsilon, \mu), \lambda(\varepsilon, \mu)$  are sufficiently stable, see Chapter 5 of book [23] for details, we can write that the Fréchet derivative of the Tikhonov functional is the function  $J'(\varepsilon, \mu, E(\varepsilon, \mu))$  which is defined as

$$(4.12) \quad \begin{aligned} J'(\varepsilon, \mu) &:= J'(\varepsilon, \mu, E(\varepsilon, \mu)) = \frac{\partial J}{\partial \varepsilon}(\varepsilon, \mu, E(\varepsilon, \mu)) + \frac{\partial J}{\partial \mu}(\varepsilon, \mu, E(\varepsilon, \mu)) \\ &= \frac{\partial L}{\partial \varepsilon}(u(\varepsilon, \mu)) + \frac{\partial L}{\partial \mu}(u(\varepsilon, \mu)). \end{aligned}$$

Inserting (4.8) and (4.9) into (4.12), we get

$$(4.13) \quad \begin{aligned} J'(\varepsilon, \mu)(x) &:= J'(\varepsilon, \mu, E(\varepsilon, \mu))(x) = - \int_0^T \partial_t \lambda \partial_t E(x, t) dt - \lambda(x, 0) f_1(x) \\ &\quad + s \int_0^T (\nabla \cdot E)(\nabla \cdot \lambda)(x, t) dt + \gamma_1(\varepsilon - \varepsilon_0)(x) \\ &\quad - \int_0^T (\mu^{-2} \nabla \times E)(\nabla \times \lambda)(x, t) dt + \gamma_2(\mu - \mu_0)(x). \end{aligned}$$

## 5. FINITE ELEMENT METHOD

**5.1. Finite element spaces.** For computations we discretize  $\Omega_{\text{FEM}} \times (0, T)$  in space and time. For discretization in space we denote by  $K_h = \{K\}$  a partition of the domain  $\Omega_{\text{FEM}}$  into tetrahedra  $K$  in  $\mathbb{R}^3$  or triangles in  $\mathbb{R}^2$ . We discretize the time interval  $(0, T)$  into subintervals  $J = (t_{k-1}, t_k]$  of uniform length  $\tau = t_k - t_{k-1}$  and denote the time partition by  $J_\tau = \{J\}$ . In our finite element space mesh  $K_h$  the elements  $K$  are such that

$$K_h = \bigcup_{K \in K_h} K = K_1 \cup K_2 \dots \cup K_l,$$

where  $l$  is the total number of elements  $K$  in  $\overline{\Omega}$ .

Similarly to [17] we introduce the mesh function  $h = h(x)$  which is a piecewise-constant function such that

$$(5.1) \quad h|_K = h_K \quad \forall K \in K_h,$$

where  $h_K$  is the diameter of  $K$  which we define as the longest side of  $K$ . Let  $r'$  be the radius of the maximal circle/sphere contained in the element  $K$ . For every element  $K \in K_h$  we assume the shape regularity assumption

$$(5.2) \quad a_1 \leq h_K \leq r' a_2; \quad a_1, a_2 = \text{const.} > 0.$$

To formulate the finite element method for (4.5), we define the finite element spaces. First we introduce the finite element trial space  $W_h^E$  for every component of the electric field  $E$  defined by

$$W_h^E := \{w \in H_E^1: w|_{K \times J} \in P_1(K) \times P_1(J) \quad \forall K \in K_h, \quad \forall J \in J_\tau\},$$

where  $P_1(K)$  and  $P_1(J)$  denote the set of linear functions on  $K$  and  $J$ , respectively. We also introduce the finite element test space  $W_h^\lambda$  defined by

$$W_h^\lambda := \{w \in H_\lambda^1: w|_{K \times J} \in P_1(K) \times P_1(J) \quad \forall K \in K_h, \quad \forall J \in J_\tau\}.$$

To approximate the functions  $\mu(x)$  and  $\varepsilon(x)$  we will use the space of piecewise constant functions  $V_h \subset L^2(\Omega)$ ,

$$V_h := \{u \in L^2(\Omega): u|_K \in P_0(K) \quad \forall K \in K_h\},$$

where  $P_0(K)$  is the space of piecewise constant functions on  $K$ . In some numerical experiments we will use also the space of piecewise linear functions  $W_h \subset H^1(\Omega)$ ,

$$(5.3) \quad W_h = \{v(x) \in H^1(\Omega): v|_K \in P_1(K) \quad \forall K \in K_h\}.$$

In a general case we allow the functions  $\varepsilon(x), \mu(x)$  to be discontinuous, see [22]. Let  $F_h$  be the set of all faces of elements in  $K_h$  such that  $F_h := F_h^I \cup F_h^B$ , where  $F_h^I$  is the set of all interior faces and  $F_h^B$  is the set of all boundary faces of elements in  $K_h$ . Let  $f \in F_h^I$  be the internal face of the nonempty intersection of the boundaries of two neighboring elements  $K^+$  and  $K^-$ . We denote the jump of the function  $v_h$  computed from the two neighboring elements  $K^+$  and  $K^-$  sharing the common side  $f$  as

$$(5.4) \quad [v_h] = v_h^+ - v_h^-,$$

and the jump of the normal component  $v_h$  across the side  $f$  as

$$(5.5) \quad [[v_h]] = v_h^+ \cdot n^+ + v_h^- \cdot n^-,$$

where  $n^+, n^-$  are the unit outward normals on  $f^+, f^-$ , respectively.

Let  $P_h$  be the  $L^2(\Omega)$ -orthogonal projection. We define by  $f_h^I$  the standard nodal interpolant [17] of  $f$  into the space of continuous piecewise-linear functions on the mesh  $K_h$ . Then by one of the properties of the orthogonal projection we have

$$(5.6) \quad \|f - P_h f\|_{L^2(\Omega)} \leq \|f - f_h^I\|_{L^2(\Omega)}.$$

It follows from [29] that

$$(5.7) \quad \|f - P_h f\|_{L^2(\Omega)} \leq C_I h \|f\|_{H^1(\Omega)} \quad \forall f \in H^1(\Omega),$$

where  $C_I = C_I(\Omega)$  is a positive constant depending only on the domain  $\Omega$ .

**5.2. A finite element method for optimization problem.** To formulate the finite element method for (4.5) we define the space  $U_h = W_h^E \times W_h^\lambda \times V_h \times V_h$ . The finite element method reads: Find  $u_h \in U_h$  such that

$$(5.8) \quad L'(u_h)(\bar{u}) = 0 \quad \forall \bar{u} \in U_h.$$

To be more precise, the equation (5.8) expresses that the finite element method for the forward problem (3.1) in  $\Omega_{\text{FEM}}$  for continuous  $(\varepsilon, \mu)$  will be: find  $E_h = (E_{1h}, E_{2h}, E_{3h}) \in W_h^E$  such that for all  $\bar{\lambda} \in W_h^\lambda$  and for the known  $(\varepsilon_h, \mu_h) \in V_h \times V_h$

$$(5.9) \quad -\left(\left(\varepsilon_h \frac{\partial \bar{\lambda}}{\partial t}, \frac{\partial E_h}{\partial t}\right)\right) - (\varepsilon_h f_1, \bar{\lambda}(x, 0))_\Omega + ((\mu_h^{-1} \nabla \times E_h, \nabla \times \bar{\lambda}))_{\Omega_T} \\ + s((\nabla \cdot (\varepsilon_h E_h), \nabla \cdot \bar{\lambda}))_{\Omega_T} - ((\bar{\lambda}, p(t)))_{S_{1,1}} + ((\bar{\lambda}, \partial_t E_h))_{S_{1,2}} \\ + ((\bar{\lambda}, \partial_t E_h))_{S_2} = 0 \quad \forall \bar{\lambda} \in H_\lambda^1(\Omega_T),$$

and the finite element method for the adjoint problem (4.10) in  $\Omega_{\text{FEM}}$  for continuous  $(\varepsilon, \mu)$  reads: find  $\lambda_h = (\lambda_{h1}, \lambda_{h2}, \lambda_{h3}) \in W_h^\lambda$  such that for the computed approximation  $E_h = (E_{1h}, E_{2h}, E_{3h}) \in W_h^E$  of (5.9) and for all  $\bar{E} \in W_h^E$  and for the known  $(\varepsilon_h, \mu_h) \in V_h \times V_h$

$$(5.10) \quad (((E_h - \tilde{E})|_{S_T z_\delta}, \bar{E})) - ((\varepsilon_h \partial_t \lambda_h, \partial_t \bar{E}))_{\Omega_T} + ((\mu_h^{-1} \nabla \times \lambda_h, \nabla \times \bar{E}))_{\Omega_T} \\ + s((\nabla \cdot \lambda_h, \nabla \cdot (\varepsilon_h \bar{E}))_{\Omega_T} - ((\partial_t \lambda_h, \bar{E}))_{S_{1,2} \cup S_2} \\ - (\varepsilon_h \bar{E}(x, 0), \partial_t \lambda_h(x, 0)) = 0 \quad \forall \bar{E} \in H_E^1(\Omega_T).$$

A similar finite element method for the forward and adjoint problems can be written for discontinuous functions  $\varepsilon$ ,  $\mu$  which will include additional terms with jumps for computation of coefficients. In our work similarly to [13] we compute the discontinuities of coefficients  $\varepsilon$  and  $\mu$  by computing the jumps from the two neighboring elements, see (5.4) and (5.5) for definitions of jumps.

Since we are usually working in finite dimensional spaces  $U_h$  and  $U_h \subset U^1$  as a set,  $U_h$  is a discrete analogue of the space  $U^1$ . It is well known that in finite dimensional spaces all norms are equivalent, and in our computations we compute approximations of smooth functions  $\varepsilon(x), \mu(x)$  in the space  $V_h$ .

**5.3. Fully discrete scheme.** To write fully discrete schemes for (5.9) and (5.10) we expand  $E_h$  and  $\lambda_h$  in terms of the standard continuous piecewise linear functions  $\{\varphi_i(x)\}_{i=1}^M$  in space and  $\{\psi_k(t)\}_{k=1}^N$  in time, respectively, as

$$E_h(x, t) = \sum_{k=1}^N \sum_{i=1}^M \mathbf{E}_h \varphi_i(x) \psi_k(t),$$

$$\lambda_h(x, t) = \sum_{k=1}^N \sum_{i=1}^M f \boldsymbol{\lambda}_h \varphi_i(x) \psi_k(t),$$

where  $\mathbf{E}_h := E_{h_{i,k}}$  and  $\boldsymbol{\lambda}_h := \lambda_{h_{i,k}}$  denote the unknown coefficients at the point  $x_i \in K_h$  and the time level  $t_k \in J_\tau$ , substitute them into (5.9) and (5.10) to obtain the following system of linear equations:

$$(5.11) \quad M(\mathbf{E}^{k+1} - 2\mathbf{E}^k + \mathbf{E}^{k-1}) = -\tau^2 K \mathbf{E}^k - s\tau^2 C \mathbf{E}^k + \tau^2 F^k + \tau^2 P^k$$

$$- \frac{1}{2} \tau (MD) \cdot (\mathbf{E}^{k+1} - \mathbf{E}^{k-1}),$$

$$M(\boldsymbol{\lambda}^{k+1} - 2\boldsymbol{\lambda}^k + \boldsymbol{\lambda}^{k-1}) = -\tau^2 S^k - \tau^2 K \boldsymbol{\lambda}^k - s\tau^2 C \boldsymbol{\lambda}^k$$

$$+ \frac{1}{2} \tau (MD) \cdot (\boldsymbol{\lambda}^{k+1} - \boldsymbol{\lambda}^{k-1}) + \tau^2 (D\boldsymbol{\lambda})^k.$$

Here,  $M$  is the block mass matrix in space and  $MD$  is the block mass matrix in space corresponding to the elements on the boundaries  $\partial_1\Omega, \partial_2\Omega$ ,  $K$  is the block stiffness matrix corresponding to the rotation term,  $C$  is the stiffness matrix corresponding to the divergence term,  $F^k, P^k, D\boldsymbol{\lambda}^k, S^k$  are load vectors at time level  $t_k$ ,  $\mathbf{E}^k$  and  $\boldsymbol{\lambda}^k$  denote the nodal values of  $\mathbf{E}_h$  and  $\boldsymbol{\lambda}_h$ , respectively, at time level  $t_k$ , and  $\tau$  is the time step. We refer to [5] for details of derivation of these matrices.

Let us define the mapping  $F_K$  for the reference element  $\widehat{K}$  such that  $F_K(\widehat{K}) = K$  and let  $\widehat{\varphi}$  be the piecewise linear local basis function on the reference element  $\widehat{K}$  such that  $\varphi \circ F_K = \widehat{\varphi}$ . Then the explicit formulas for the entries in system (5.11) at each

element  $K$  can be given as

$$\begin{aligned}
M_{i,j}^K &= (\varepsilon_h \varphi_i \circ F_K, \varphi_j \circ F_K)_K, \\
K_{i,j}^K &= (\mu_h^{-1} \nabla \times \varphi_i \circ F_K, \nabla \times \varphi_j \circ F_K)_K, \\
C_{i,j}^K &= (\nabla \cdot (\varepsilon_h \varphi_i) \circ F_K, \nabla \cdot \varphi_j \circ F_K)_K, \\
S_j^K &= ((E_h - \tilde{E})_{S_T z_\sigma}, \varphi_j \circ F_K)_K, \\
F_j^K &= (\varepsilon_h f_1, \varphi_j \circ F_K)_K, \\
P_j^K &= (p, \varphi_j \circ F_K)_{\partial_1 \Omega_K}, \\
MD_j^K &= (\varphi_i \circ F_K, \varphi_j \circ F_K)_{\partial_1 \Omega_K \cup \partial_2 \Omega_K}, \\
D\lambda_j^K &= (\varepsilon_h \partial_t \lambda_h(x, 0), \varphi_j \circ F_K)_K,
\end{aligned}$$

where  $(\cdot, \cdot)_K$  denotes the  $L^2(K)$  scalar product, and  $\partial_1 \Omega_K, \partial_2 \Omega_K$  are boundaries  $\partial K$  of elements  $K$ , which belong to  $\partial_1 \Omega, \partial_2 \Omega$ , respectively.

To obtain an explicit scheme, we approximate  $M$  by the lumped mass matrix  $M^L$  (for further details, see [14]). Next, we multiply (5.11) by  $(M^L)^{-1}$  and get the following explicit method:

$$\begin{aligned}
(5.12) \quad & (I + \frac{1}{2}\tau(M^L)^{-1}MD)\mathbf{E}^{k+1} \\
&= 2\mathbf{E}^k - \tau^2(M^L)^{-1}K\mathbf{E}^k + \tau^2(M^L)^{-1}F^k + \tau^2(M^L)^{-1}P^k \\
&\quad + \frac{1}{2}\tau(M^L)^{-1}(MD)\mathbf{E}^{k-1} - s\tau^2(M^L)^{-1}C\mathbf{E}^k - \mathbf{E}^{k-1}, \\
& (I + \frac{1}{2}\tau(M^L)^{-1}MD)\boldsymbol{\lambda}^{k-1} \\
&= -\tau^2(M^L)^{-1}S^k + 2\boldsymbol{\lambda}^k - \tau^2(M^L)^{-1}K\boldsymbol{\lambda}^k - s\tau^2(M^L)^{-1}C\boldsymbol{\lambda}^k \\
&\quad + \tau^2(M^L)^{-1}(D\boldsymbol{\lambda})^k - \boldsymbol{\lambda}^{k+1} + \frac{1}{2}\tau(M^L)^{-1}(MD)\boldsymbol{\lambda}^{k+1}.
\end{aligned}$$

In the case of the domain decomposition FEM/FDM method when the schemes above are used only in  $\Omega_{\text{FEM}}$  we have

$$\begin{aligned}
(5.13) \quad & \mathbf{E}^{k+1} = 2\mathbf{E}^k - \tau^2(M^L)^{-1}K\mathbf{E}^k + \tau^2(M^L)^{-1}F^k \\
&\quad + \tau^2(M^L)^{-1}P^k - s\tau^2(M^L)^{-1}C\mathbf{E}^k - \mathbf{E}^{k-1}, \\
& \boldsymbol{\lambda}^{k-1} = -\tau^2(M^L)^{-1}S^k + 2\boldsymbol{\lambda}^k - \tau^2(M^L)^{-1}K\boldsymbol{\lambda}^k \\
&\quad - s\tau^2(M^L)^{-1}C\boldsymbol{\lambda}^k + \tau^2(M^L)^{-1}D\boldsymbol{\lambda} - \boldsymbol{\lambda}^{k+1}.
\end{aligned}$$

## 6. RELAXATION PROPERTY OF MESH REFINEMENTS

In this section we reformulate results of [9] for the case of our IP. For simplicity, we shall sometimes write  $\|\cdot\|$  for the  $L^2$ -norm.

We use the theory of ill-posed problems [32], [31] and introduce the noise level  $\delta$  in the function  $\tilde{E}(x, t)$  in the Tikhonov functional (4.1). This means that

$$(6.1) \quad \tilde{E}(x, t) = \tilde{E}^*(x, t) + \tilde{E}_\delta(x, t); \quad \tilde{E}^*, \tilde{E}_\delta \in L^2(S_T) = H_2,$$

where  $\tilde{E}^*(x, t)$  is the exact data corresponding to the exact function  $z^* = (\varepsilon^*, \mu^*)$ , and the function  $\tilde{E}_\delta(x, t)$  represents the error in these data. In other words, we can write

$$(6.2) \quad \|\tilde{E}_\delta\|_{L^2(S_T)} \leq \delta.$$

The question of stability and uniqueness of our IP is addressed in [6], [11], which is needed in the local strong convexity theorem formulated below. Let  $H_1$  be the finite dimensional linear space. Let  $Y$  be the set of admissible functions  $(\varepsilon, \mu)$  which we defined in (3.2), and let  $Y_1 := Y \cap H_1$  with  $G := \bar{Y}_1$ . We introduce now the operator  $F: G \rightarrow H_2$  corresponding to the Tikhonov functional (4.1) such that

$$(6.3) \quad F(z)(x, t) := F(\varepsilon, \mu)(x, t) = (E(x, t, \varepsilon, \mu) - \tilde{E})^2 z_\delta(t) \quad \forall (x, t) \in S_T,$$

where  $E(x, t, \varepsilon, \mu) := E(x, t)$  is the weak solution of the forward problem (3.1) and thus depends on  $\varepsilon$  and  $\mu$ . Here,  $z = (\varepsilon, \mu)$  and  $z_\delta(t)$  is a cut-off function chosen as in [6].

We now assume that the operator  $F(z)(x, t)$  which we defined in (6.3) is one-to-one. Let us denote by

$$(6.4) \quad V_d(z) = \{z' \in H_1: \|z' - z\| < d \quad \forall z = (\varepsilon, \mu) \in H_1\}$$

the neighborhood of  $z$  of the diameter  $d$ . We also assume that the operator  $F$  is Lipschitz continuous, which means that for  $N_1, N_2 > 0$

$$(6.5) \quad \|F'(z)\| \leq N_1, \|F'(z_1) - F'(z_2)\| \leq N_2 \|z_1 - z_2\| \quad \forall z_1, z_2 \in V_1(z^*).$$

Let the constant  $D = D(N_1, N_2) = \text{const.} > 0$  be such that

$$(6.6) \quad \|J'(z_1) - J'(z_2)\| \leq D \|z_1 - z_2\| \quad \forall z_1, z_2 \in V_1(z^*),$$

where  $(\varepsilon^*, \mu^*)$  is the exact solution of the equation  $F(\varepsilon^*, \mu^*) = 0$ . Similarly to [9], we assume that

$$(6.7) \quad \begin{aligned} \|\varepsilon_0 - \varepsilon^*\| &\leq \delta^{\nu_1}, \quad \nu_1 = \text{const.} \in (0, 1), \\ \|\mu_0 - \mu^*\| &\leq \delta^{\nu_2}, \quad \nu_2 = \text{const.} \in (0, 1), \\ \gamma_1 &= \delta^{\zeta_1}, \quad \zeta_1 = \text{const.} \in (0, \min(\nu_1, 2(1 - \nu_1))), \\ \gamma_2 &= \delta^{\zeta_2}, \quad \zeta_2 = \text{const.} \in (0, \min(\nu_2, 2(1 - \nu_2))), \end{aligned}$$

which in closed form can be written as

$$(6.8) \quad \|z_0 - z^*\| \leq \delta^{(\nu_1, \nu_2)}, \quad z_0 = (\varepsilon_0, \mu_0), \quad (\nu_1, \nu_2) = \text{const.} \in (0, 1),$$

$$(6.9) \quad (\gamma_1, \gamma_2) = \delta^{(\zeta_1, \zeta_2)}, \quad (\zeta_1, \zeta_2) = \text{const.} \in (0, \min((\nu_1, \nu_2), 2(1 - (\nu_1, \nu_2))))),$$

where  $(\gamma_1, \gamma_2)$  are regularization parameters in (4.1). Equation (6.8) means that we assume that all initial guesses  $z_0 = (\varepsilon_0, \mu_0)$  are located in a sufficiently small neighborhood  $V_{\delta^{\mu_1}}(z^*)$  of the exact solution  $z^* = (\varepsilon^*, \mu^*)$ . Conditions (6.9) imply that  $(z^*, z_0)$  belong to an appropriate neighborhood of the regularized solution of the functional (4.1), see proofs in Lemmas 2.1 and 3.2 of [9].

Below we reformulate Theorem 1.9.1.2 of [8] for the Tikhonov functional (4.1). Different proofs of it can be found in [8] and in [9] and are immediately applied to our IP. We note here that if functions  $(\varepsilon, \mu) \in H_1$  satisfy conditions (3.2) then  $(\varepsilon, \mu) \in \text{Int}(G)$ .

**Theorem 1.** *Let  $\Omega \subset \mathbb{R}^3$  be a convex bounded domain with the boundary  $\partial\Omega \in C^3$ . Suppose that conditions (6.1) and (6.2) hold. Let the function  $E(x, t) \in H^2(\Omega_T)$  in the Tikhonov functional (4.1) be the solution of the forward problem (3.1) for the functions  $(\varepsilon, \mu) \in G$ . Assume that there exist exact solutions  $(\varepsilon^*, \mu^*) \in G$  of the equation  $F(\varepsilon^*, \mu^*) = 0$  for the case of the exact data  $\tilde{E}^*$  in (6.1). Let the regularization parameters  $(\gamma_1, \gamma_2)$  in (4.1) be such that*

$$(\gamma_1, \gamma_2) = (\gamma_1, \gamma_2)(\delta) = \delta^{2(\nu_1, \nu_2)}, \quad (\nu_1, \nu_2) = \text{const.} \in (0, \frac{1}{4}) \quad \forall \delta \in (0, 1).$$

*Let  $z_0 = (\varepsilon_0, \mu_0)$  satisfy (6.8). Then the Tikhonov functional (4.1) is strongly convex in the neighborhood  $V_{(\gamma_1, \gamma_2)(\delta)}(\varepsilon^*, \mu^*)$  with the strong convexity constants  $(\alpha_1, \alpha_2) = (\gamma_1, \gamma_2)/2$ . The strong convexity property can be also written as*

$$(6.10) \quad \|z_1 - z_2\|^2 \leq \frac{2}{\delta^{2(\nu_1, \nu_2)}} (J'(z_1) - J'(z_2), z_1 - z_2) \quad \forall z_1 = (\varepsilon_1, \mu_1), \quad z_2 = (\varepsilon_2, \mu_2) \in H_1.$$

Alternatively, using the expression for the Fréchet derivative given in (4.12), we can write (6.10) as

$$(6.11) \quad \begin{aligned} \|\varepsilon_1 - \varepsilon_2\|^2 &\leq \frac{2}{\delta^2\nu_1} (J'_\varepsilon(\varepsilon_1, \mu_1) - J'_\varepsilon(\varepsilon_2, \mu_2), \varepsilon_1 - \varepsilon_2) \quad \forall (\varepsilon_1, \mu_1), (\varepsilon_2, \mu_2) \in H_1, \\ \|\mu_1 - \mu_2\|^2 &\leq \frac{2}{\delta^2\nu_2} (J'_\mu(\varepsilon_1, \mu_1) - J'_\mu(\varepsilon_2, \mu_2), \mu_1 - \mu_2) \quad \forall (\varepsilon_1, \mu_1), (\varepsilon_2, \mu_2) \in H_1, \end{aligned}$$

where  $(\cdot, \cdot)$  is the  $L^2(\Omega)$  inner product. Next, there exists a unique regularized solution  $(\varepsilon_{\gamma_1}, \mu_{\gamma_2})$  of the functional (4.1) such that  $(\varepsilon_{\gamma_1}, \mu_{\gamma_2}) \in V_{\delta^3(\nu_1, \nu_2)/3}(\varepsilon^*, \mu^*)$ . The gradient method of the minimization of the functional (4.1) which starts at  $(\varepsilon_0, \mu_0)$  converges to the regularized solution of this functional. Furthermore,

$$(6.12) \quad \begin{aligned} \|\varepsilon_{\gamma_1} - \varepsilon^*\| &\leq \Theta_1 \|\varepsilon_0 - \varepsilon^*\|, \quad \Theta_1 \in (0, 1), \\ \|\mu_{\gamma_2} - \mu^*\| &\leq \Theta_2 \|\mu_0 - \mu^*\|, \quad \Theta_2 \in (0, 1). \end{aligned}$$

The property (6.12) means that the regularized solution of the Tikhonov functional (4.1) provides a better accuracy than the initial guess  $(\varepsilon_0, \mu_0)$  if it satisfies condition (6.8). The next theorem presents an estimate of the norm  $\|(\varepsilon, \mu) - (\varepsilon_{\gamma_1}, \mu_{\gamma_2})\|$  via the norm of the Fréchet derivative of the Tikhonov functional (4.1).

**Theorem 2.** Assume that the conditions of Theorem 1 hold. Then for any functions  $(\varepsilon, \mu) \in V_{(\gamma_1, \gamma_2)(\delta)}(\varepsilon^*, \mu^*)$  the following error estimate holds:

$$(6.13) \quad \|(\varepsilon, \mu) - (\varepsilon_{\gamma_1(\delta)}, \mu_{\gamma_2(\delta)})\| \leq \frac{2}{\delta^2(\nu_1, \nu_2)} \|P_h J'(\varepsilon, \mu)\| \leq \frac{2}{\delta^2(\nu_1, \nu_2)} \|J'(\varepsilon, \mu)\|,$$

which explicitly can be written as

$$(6.14) \quad \begin{aligned} \|\varepsilon - \varepsilon_{\gamma_1(\delta)}\| &\leq \frac{2}{\delta^2\nu_1} \|P_h J'_\varepsilon(\varepsilon, \mu)\| \leq \frac{2}{\delta^2\nu_1} \|J'_\varepsilon(\varepsilon, \mu)\| = \frac{2}{\delta^2\nu_1} \|L'_\varepsilon(u(\varepsilon, \mu))\|, \\ \|\mu - \mu_{\gamma_2(\delta)}\| &\leq \frac{2}{\delta^2\nu_2} \|P_h J'_\mu(\varepsilon, \mu)\| \leq \frac{2}{\delta^2\nu_2} \|J'_\mu(\varepsilon, \mu)\| = \frac{2}{\delta^2\nu_2} \|L'_\mu(u(\varepsilon, \mu))\|, \end{aligned}$$

where  $(\varepsilon_{\gamma_1(\delta)}, \mu_{\gamma_2(\delta)})$  is the minimizer of the Tikhonov functional (4.1) computed with regularization parameters  $(\gamma_1(\delta), \gamma_2(\delta))$  and  $P_h: L^2(\Omega) \rightarrow H_1$  is the operator of orthogonal projection of the space  $L^2(\Omega)$  onto its subspace  $H_1$ .

**Proof.** Since  $(\varepsilon_{\gamma_1}, \mu_{\gamma_2}) := (\varepsilon_{\gamma_1(\delta)}, \mu_{\gamma_2(\delta)})$  is the minimizer of the functional (4.1) on the set  $G$  and  $(\varepsilon_{\gamma_1}, \mu_{\gamma_2}) \in \text{Int}(G)$ , hence  $P_h J'(\varepsilon_{\gamma_1}, \mu_{\gamma_2}) = 0$ , or

$$(6.15) \quad P_h J'_\varepsilon(\varepsilon_{\gamma_1}, \mu_{\gamma_2}) = 0, \quad P_h J'_\mu(\varepsilon_{\gamma_1}, \mu_{\gamma_2}) = 0.$$

Similarly to Theorem 4.11.2 of [8], since  $(\varepsilon, \mu) - (\varepsilon_{\gamma_1}, \mu_{\gamma_2}) \in H_1$ , we have

$$\begin{aligned} & (J'(\varepsilon, \mu) - J'(\varepsilon_{\gamma_1}, \mu_{\gamma_2}), (\varepsilon, \mu) - (\varepsilon_{\gamma_1}, \mu_{\gamma_2})) \\ &= (P_h J'(\varepsilon, \mu) - P_h J'(\varepsilon_{\gamma_1}, \mu_{\gamma_2}), (\varepsilon, \mu) - (\varepsilon_{\gamma_1}, \mu_{\gamma_2})). \end{aligned}$$

Hence, using (6.10) and (6.15), we can write

$$\begin{aligned} \|(\varepsilon, \mu) - (\varepsilon_{\gamma_1}, \mu_{\gamma_2})\|^2 &\leq \frac{2}{\delta^{2(\nu_1, \nu_2)}} (J'(\varepsilon, \mu) - J'(\varepsilon_{\gamma_1}, \mu_{\gamma_2}), (\varepsilon, \mu) - (\varepsilon_{\gamma_1}, \mu_{\gamma_2})) \\ &= \frac{2}{\delta^{2(\nu_1, \nu_2)}} (P_h J'(\varepsilon, \mu) - P_h J'(\varepsilon_{\gamma_1}, \mu_{\gamma_2}), (\varepsilon, \mu) - (\varepsilon_{\gamma_1}, \mu_{\gamma_2})) \\ &= \frac{2}{\delta^{2(\nu_1, \nu_2)}} (P_h J'(\varepsilon, \mu), (\varepsilon, \mu) - (\varepsilon_{\gamma_1}, \mu_{\gamma_2})) \\ &\leq \frac{2}{\delta^{2(\nu_1, \nu_2)}} \|P_h J'(\varepsilon, \mu)\| \cdot \|(\varepsilon, \mu) - (\varepsilon_{\gamma_1}, \mu_{\gamma_2})\|. \end{aligned}$$

Thus, from the expression above we get

$$\|(\varepsilon, \mu) - (\varepsilon_{\gamma_1}, \mu_{\gamma_2})\|^2 \leq \frac{2}{\delta^{2(\nu_1, \nu_2)}} \|P_h J'(\varepsilon, \mu)\| \cdot \|(\varepsilon, \mu) - (\varepsilon_{\gamma_1}, \mu_{\gamma_2})\|.$$

We now divide the expression above by  $\|(\varepsilon, \mu) - (\varepsilon_{\gamma_1}, \mu_{\gamma_2})\|$ . Using the fact that

$$\|P_h J'(\varepsilon, \mu)\| \leq \|J'(\varepsilon, \mu)\|,$$

we obtain (6.13), and using the definition of the derivative of the Tikhonov functional (4.12), we get (6.14), where the explicit entries of  $L'_\varepsilon(u(\varepsilon, \mu))$ ,  $L'_\mu(u(\varepsilon, \mu))$  are given by (4.8), (4.9), respectively.  $\square$

Below we reformulate Lemmas 2.1 and 3.2 of [9] for the case of the Tikhonov functional (4.1).

**Theorem 3.** *Let the assumptions of Theorems 1 and 2 hold. Let  $\|(\varepsilon^*, \mu^*)\| \leq C$ , with a given constant  $C$ . We define by  $M_n \subset H_1$  the subspace which is obtained after  $n$  mesh refinements of the mesh  $K_h$ . Let  $h_n$  be the mesh function on  $M_n$  as defined in Section 5. Then there exists a unique minimizer  $(\varepsilon_n, \mu_n) \in G \cap M_n$  of the Tikhonov functional (4.1) such that the following inequalities hold:*

$$(6.16) \quad \begin{aligned} \|\varepsilon_n - \varepsilon_{\gamma_1(\delta)}\| &\leq \frac{2}{\delta^{2\nu_1}} \|J'_\varepsilon(\varepsilon, \mu)\|, \\ \|\mu_n - \mu_{\gamma_2(\delta)}\| &\leq \frac{2}{\delta^{2\nu_2}} \|J'_\mu(\varepsilon, \mu)\|. \end{aligned}$$

Now we present the relaxation property of mesh refinements for the Tikhonov functional (4.1) which follows from Theorem 4.1 of [9].

**Theorem 4.** *Let the assumptions of Theorems 2 and 3 hold. Let  $(\varepsilon_n, \mu_n) \in V_{\delta^3\mu}(\varepsilon^*, \mu^*) \cap M_n$  be the minimizer of the Tikhonov functional (4.1) on the set  $G \cap M_n$ . The existence of the minimizer is guaranteed by Theorem 3. Assume that the regularized solution satisfies  $(\varepsilon, \mu) \neq (\varepsilon_n, \mu_n)$ , which means that  $(\varepsilon, \mu) \notin M_n$ . Then the relaxation properties*

$$\begin{aligned} \|\varepsilon_{n+1} - \varepsilon\| &\leq \eta_{1,n} \|\varepsilon_n - \varepsilon\|, \\ \|\mu_{n+1} - \mu\| &\leq \eta_{2,n} \|\mu_n - \mu\| \end{aligned}$$

hold for  $\eta_{1,n}, \eta_{2,n} \in (0, 1)$ .

## 7. GENERAL FRAMEWORK OF A POSTERIORI ERROR ESTIMATE

In this section we briefly present a posteriori error estimates for three kinds of errors:

- ▷ for the error  $|L(u) - L(u_h)|$  in the Lagrangian (4.3);
- ▷ for the error  $|J(\varepsilon, \mu) - J(\varepsilon_h, \mu_h)|$  in the Tikhonov functional (4.1);
- ▷ for the errors  $|\varepsilon - \varepsilon_h|$  and  $|\mu - \mu_h|$  in the regularized solutions  $\varepsilon, \mu$  of this functional.

Here,  $u_h, \varepsilon_h, \mu_h$  are finite element approximations of the functions  $u, \varepsilon, \mu$ , respectively. An a posteriori error estimate in the Lagrangian was already derived in [4] for the case when only the function  $\varepsilon(x)$  in system (3.1) is unknown. In [25], [24] a posteriori error estimates were derived in the Lagrangian which corresponds to the modified system (3.1) for  $\mu = 1$ . An a posteriori error in the Lagrangian (4.3) can be derived directly from the a posteriori error estimate presented in [4] and thus, all details of this derivation are not presented here.

However, to make clear how a posteriori errors in the Lagrangian and in the Tikhonov functional can be obtained, we present the general framework for them. First we note that

$$\begin{aligned} (7.1) \quad J(\varepsilon, \mu) - J(\varepsilon_h, \mu_h) &= J'_\varepsilon(\varepsilon_h, \mu_h)(\varepsilon - \varepsilon_h) + J'_\mu(\varepsilon_h, \mu_h)(\mu - \mu_h) \\ &\quad + R(\varepsilon, \varepsilon_h) + R(\mu, \mu_h), \\ L(u) - L(u_h) &= L'(u_h)(u - u_h) + R(u, u_h), \end{aligned}$$

where  $R(\varepsilon, \varepsilon_h), R(\mu, \mu_h), R(u, u_h)$  are the remainders of the second order. We assume that  $(\varepsilon_h, \mu_h)$  are located in a small neighborhood of the regularized solutions  $(\varepsilon, \mu)$ , correspondingly. Thus, since the terms  $R(u, u_h), R(\varepsilon, \varepsilon_h), R(\mu, \mu_h)$  are of the second order, they will be small and we can neglect them in (7.1).

We now use the splitting

$$(7.2) \quad \begin{aligned} u - u_h &= (u - u_h^I) + (u_h^I - u_h), \\ \varepsilon - \varepsilon_h &= (\varepsilon - \varepsilon_h^I) + (\varepsilon_h^I - \varepsilon_h), \\ \mu - \mu_h &= (\mu - \mu_h^I) + (\mu_h^I - \mu_h), \end{aligned}$$

together with the Galerkin orthogonality principle

$$(7.3) \quad \begin{aligned} L'(u_h)(\bar{u}) &= 0 \quad \forall \bar{u} \in U_h, \\ J'(z_h)(b) &= 0 \quad \forall b \in V_h, \end{aligned}$$

insert (7.2) into (7.1) and get the error representations

$$(7.4) \quad \begin{aligned} L(u) - L(u_h) &\approx L'(u_h)(u - u_h^I), \\ J(\varepsilon, \mu) - J(\varepsilon_h, \mu_h) &\approx J'_\varepsilon(\varepsilon_h, \mu_h)(\varepsilon - \varepsilon_h^I) + J'_\mu(\varepsilon_h, \mu_h)(\mu - \mu_h^I). \end{aligned}$$

In (7.2), (7.4) the functions  $u_h^I \in U_h$  and  $\varepsilon_h^I, \mu_h^I \in V_h$  denote the interpolants of  $u$ ,  $\varepsilon$ ,  $\mu$ , respectively.

Using (7.4) we conclude that the a posteriori error estimate in the Lagrangian involves the derivative of the Lagrangian  $L'(u_h)$  which we define as a residual, multiplied by the weights  $u - u_h^I$ . Similarly, the a posteriori error estimate in the Tikhonov functional involves the derivatives of the Tikhonov functional  $J'_\varepsilon(\varepsilon_h, \mu_h)$  and  $J'_\mu(\varepsilon_h, \mu_h)$  which represent the residuals, multiplied by the weights  $\varepsilon - \varepsilon_h^I$  and  $\mu - \mu_h^I$ , correspondingly.

To derive the errors  $|\varepsilon - \varepsilon_h|$  and  $|\mu - \mu_h|$  in the regularized solutions  $\varepsilon, \mu$  of the functional (4.1) we will use the convexity property of the Tikhonov functional together with the interpolation property (5.7). We will now make both the error estimates more explicit.

## 8. A POSTERIORI ERROR ESTIMATE IN THE REGULARIZED SOLUTION

In this section we formulate a theorem for a posteriori error estimates  $|\varepsilon - \varepsilon_h|$  and  $|\mu - \mu_h|$  in the regularized solution  $\varepsilon, \mu$  of the functional (4.1). In the proof we reduce the notation and denote the scalar product  $(\cdot, \cdot)_{L^2}$  as  $(\cdot, \cdot)$ , as well as we denote the norm  $\|\cdot\|_{L^2}$  as  $\|\cdot\|$ . However, if the norm should be specified, we will write it explicitly.

**Theorem 5.** *Let the assumptions of Theorems 1 and 2 hold. Let  $z_h = (\varepsilon_h, \mu_h) \in W_h$  be finite element approximations of the regularized solution  $z = (\varepsilon, \mu)$  on the finite element mesh  $K_h$ . Then there exists a constant  $D$  defined in (6.6) such that the following a posteriori error estimates hold:*

$$(8.1) \quad \begin{aligned} \|\varepsilon - \varepsilon_h\| &\leq \frac{D}{\alpha_1} C_I(h\|\varepsilon_h\| + \|[\varepsilon_h]\|) = \frac{2D}{\delta^{2\nu_1}} C_I(h\|\varepsilon_h\| + \|[\varepsilon_h]\|) \quad \forall \varepsilon_h \in V_h, \\ \|\mu - \mu_h\| &\leq \frac{D}{\alpha_2} C_I(h\|\mu_h\| + \|[\mu_h]\|) = \frac{2D}{\delta^{2\nu_2}} C_I(h\|\mu_h\| + \|[\mu_h]\|) \quad \forall \mu_h \in V_h. \end{aligned}$$

*Proof.* Let  $z_h = (\varepsilon_h, \mu_h)$  be the minimizer of the Tikhonov functional (4.1). The existence and uniqueness of this minimizer is guaranteed by Theorem 2. By Theorem 1, the functional (4.1) is strongly convex on the space  $L^2$  with the strong convexity constants  $(\alpha_1, \alpha_2) = (\gamma_1/2, \gamma_2/2)$ . This fact implies, see (6.10), that

$$(8.2) \quad (\alpha_1, \alpha_2) \|z - z_h\|_{L^2(\Omega)}^2 \leq (J'(z) - J'(z_h), z - z_h),$$

where  $J'(z_h), J'(z)$  are the Fréchet derivatives of the functional (4.1).

Using (8.2) with the splitting

$$z - z_h = (z - z_h^I) + (z_h^I - z_h),$$

where  $z_h^I$  is the standard interpolant of  $z$ , and combining it with the Galerkin orthogonality principle

$$(8.3) \quad (J'(z_h) - J'(z), z_h^I - z_h) = 0$$

such that  $(z_h, z_h^I) \in W_h$ , we obtain

$$(8.4) \quad (\alpha_1, \alpha_2) \|z - z_h\|_{L^2}^2 \leq (J'(z) - J'(z_h), z - z_h^I).$$

The right-hand side of (8.4) can be estimated using (6.6) as

$$(J'(z) - J'(z_h), z - z_h^I) \leq D \|z - z_h\| \cdot \|z - z_h^I\|.$$

Substituting the above equation into (8.4), we find that

$$(8.5) \quad \|z - z_h\| \leq \frac{D}{(\alpha_1, \alpha_2)} \|z - z_h^I\|.$$

Using the interpolation property (5.7)

$$\|z - z_h^I\|_{L^2(\Omega)} \leq C_I h \|z\|_{H^1(\Omega)},$$

we get an a posteriori error estimate for the regularized solution  $z$  with the interpolation constant  $C_I$ :

$$(8.6) \quad \|z - z_h\| \leq \frac{D}{(\alpha_1, \alpha_2)} \|z - z_h^I\| \leq \frac{D}{(\alpha_1, \alpha_2)} C_I h \|z\|_{H^1(\Omega)}.$$

We can estimate  $h\|z\|_{H^1(\Omega)}$  as

$$(8.7) \quad \begin{aligned} h\|z\|_{H^1(\Omega)} &\leq \sum_K h_K \|z\|_{H^1(K)} = \sum_K \|(z + \nabla z)\|_{L^2(K)} h_K \\ &\leq \sum_K \left( h_K \|z_h\|_{L^2(K)} + \left\| \frac{[z_h]}{h_K} h_K \right\|_{L^2(K)} \right) \\ &\leq h \|z_h\|_{L^2(\Omega)} + \sum_K (\|[z_h]\|_{L^2(K)}). \end{aligned}$$

We denote in (8.7) by  $[z_h]$  the jump of the function  $z_h$  over the element  $K$ ,  $h_K$  is the diameter of the element  $K$ . In (8.7) we also used the fact that [20]

$$(8.8) \quad |\nabla z| \leq \frac{[z_h]}{h_K}.$$

Substituting the above estimates into the right-hand side of (8.6), we get

$$\|z - z_h\| \leq \frac{D}{(\alpha_1, \alpha_2)} C_I h \|z_h\| + \frac{D}{(\alpha_1, \alpha_2)} C_I \|[z_h]\| \quad \forall z_h \in W_h.$$

Now taking into account  $z_h = (\varepsilon_h, \mu_h)$ , we get the estimates (8.1) for  $|\varepsilon - \varepsilon_h|$  and  $|\mu - \mu_h|$ , correspondingly.  $\square$

## 9. A POSTERIORI ERROR ESTIMATES FOR THE TIKHONOV FUNCTIONAL

In Theorem 2 we derived a posteriori error estimates for the error in the Tikhonov functional (4.1) obtained on the finite element mesh  $K_h$ .

**Theorem 6.** *Suppose that there exists a minimizer  $(\varepsilon, \mu) \in H^1(\Omega)$  of the Tikhonov functional (4.1) on the mesh  $K_h$ . Suppose also that there exists a finite element approximation  $z_h = (\varepsilon_h, \mu_h)$  of  $z = (\varepsilon, \mu)$  of  $J(\varepsilon, \mu)$  on the set  $W_h$  and the mesh  $K_h$  with the mesh function  $h$ . Then the following a posteriori error estimate for the error  $e = |J(\varepsilon, \mu) - J(\varepsilon_h, \mu_h)|$  in the Tikhonov functional (4.1) holds:*

$$(9.1) \quad \begin{aligned} e &= |J(\varepsilon, \mu) - J(\varepsilon_h, \mu_h)| \\ &\leq C_I (\|J'_\varepsilon(\varepsilon_h, \mu_h)\| (h\|\varepsilon_h\| + \|[ \varepsilon_h ] \|) + \|J'_\mu(\varepsilon_h, \mu_h)\| (h\|\mu_h\| + \|[ \mu_h ] \|)) \\ &= C_I (\|L'_\varepsilon(u(\varepsilon_h, \mu_h))\| (h\|\varepsilon_h\| + \|[ \varepsilon_h ] \|) + \|L'_\mu(u(\varepsilon_h, \mu_h))\| (h\|\mu_h\| + \|[ \mu_h ] \|)). \end{aligned}$$

**Proof.** By the definition of the Fréchet derivative of the Tikhonov functional (4.1) with  $z = (\varepsilon, \mu)$ ,  $z_h = (\varepsilon_h, \mu_h)$  we can write that on the mesh  $K_h$

$$(9.2) \quad J(z) - J(z_h) = J'(z_h)(z - z_h) + R(z, z_h),$$

where the remainder is  $R(z, z_h) = O((z - z_h)^2)$ ,  $(z - z_h) \rightarrow 0$  for all  $z, z_h \in W_h$  and  $J'(z_h)$  is the Fréchet derivative of the functional (4.1). We can neglect the term  $R(z, z_h)$  in the estimate (9.2), since it is small. This is because we assume that  $z_h$  is the minimizer of the Tikhonov functional on the mesh  $K_h$  and this minimizer is located in a small neighborhood of the regularized solution  $z$ . For similar results for the case of the general nonlinear operator equation we refer to [2], [9]. We again use the splitting

$$(9.3) \quad z - z_h = z - z_h^I + z_h^I - z_h$$

and the Galerkin orthogonality [17]

$$(9.4) \quad J'(z_h)(z_h^I - z_h) = 0 \quad \forall z_h^I, z_h \in W_h$$

to get

$$(9.5) \quad J(z) - J(z_h) \leq J'(z_h)(z - z_h^I),$$

where  $z_h^I$  is the standard interpolant of  $z$  on the mesh  $K_h$  [17]. Using (9.5), we can also write

$$(9.6) \quad |J(z) - J(z_h)| \leq \|J'(z_h)\| \cdot \|z - z_h^I\|,$$

where the term  $\|z - z_h^I\|$  can be estimated through the interpolation estimate

$$\|z - z_h^I\|_{L^2(\Omega)} \leq C_I \|hz\|_{H^1(\Omega)}.$$

Substituting the above estimate into (9.6), we get

$$(9.7) \quad |J(z) - J(z_h)| \leq C_I \|J'(z_h)\| \|h\| \|z\|_{H^1(\Omega)}.$$

Using (8.8), we can estimate  $h\|z\|_{H^1(\Omega)}$  similarly to (8.7) to get

$$(9.8) \quad |J(z) - J(z_h)| \leq C_I \|J'(z_h)\| (h\|z_h\| + \|[z_h]\|) \quad \forall z_h \in W_h.$$

Now taking into account  $z_h = (\varepsilon_h, \mu_h)$  and using (4.12), we get the estimate (9.1) for  $|J(\varepsilon, \mu) - J(\varepsilon_h, \mu_h)|$ . □

## 10. MESH REFINEMENT RECOMMENDATIONS

In this section we will show how to use Theorems 5 and 6 for the local mesh refinement recommendation. This recommendation will allow to improve accuracy of the reconstruction of the regularized solution  $(\varepsilon, \mu)$  of our problem IP.

Using the estimate (8.1), we observe that the main contributions of the norms of the reconstructed functions  $(\varepsilon_h, \mu_h)$  are given by neighborhoods of the points in the finite element mesh  $K_h$ , where the computed values of  $|h\varepsilon_h|$  and  $|h\mu_h|$  achieve its maximal values.

We also note that terms with the jumps in the estimate (8.1) disappear in the case of the conforming finite element meshes and with  $(\varepsilon_h, \mu_h) \in V_h$ . Our idea of the local finite element mesh refinement is that it should be refined in all neighborhoods of all points in the mesh  $K_h$ , where the functions  $|h\varepsilon_h|$  and  $|h\mu_h|$  achieve their maximum values.

Similarly, the estimate (9.1) of Theorem 6 gives us the idea where to locally refine the finite element mesh  $K_h$  to improve the accuracy in the Tikhonov functional (4.1). Using the estimate (9.1), we observe that the main contributions of the norms on the right-hand side of (9.1) are given by neighborhoods of the points in the finite element mesh  $K_h$ , where the computed values of  $|h\varepsilon_h|$ ,  $|h\mu_h|$ , as well as the computed values of  $|J'_\varepsilon(\varepsilon_h, \mu_h)|$ ,  $|J'_\mu(\varepsilon_h, \mu_h)|$  achieve its maximal values.

Recalling (4.12), (4.8), and (4.9), we have

$$(10.1) \quad J'_\varepsilon(\varepsilon_h, \mu_h)(x) = - \int_0^T (\partial_t \lambda \partial_t E)(x, t) dt + s \int_0^T (\nabla \cdot E)(\nabla \cdot \lambda)(x, t) dt \\ - \lambda(x, 0) f_1(x) + \gamma_1(\varepsilon_h - \varepsilon_0)(x), \quad x \in \Omega,$$

$$(10.2) \quad J'_\mu(\varepsilon_h, \mu_h)(x) = - \int_0^T (\mu_h^{-2} \nabla \times E \nabla \times \lambda)(x, t) dt + \gamma_2(\mu_h - \mu_0)(x), \quad x \in \Omega.$$

Thus, the second idea where to refine the finite element mesh  $K_h$  is that the neighborhoods of all points in  $K_h$ , where  $|J'_\varepsilon(\varepsilon_h, \mu_h)| + |J'_\mu(\varepsilon_h, \mu_h)|$  achieves its maximum, or both functions  $|h\varepsilon_h| + |h\mu_h|$  and  $|J'_\varepsilon(\varepsilon_h, \mu_h)| + |J'_\mu(\varepsilon_h, \mu_h)|$  achieve their maximum, should be refined. We include the term  $|h\varepsilon_h| + |h\mu_h|$  in the first mesh refinement recommendation, and the term  $|J'_\varepsilon(\varepsilon_h, \mu_h)| + |J'_\mu(\varepsilon_h, \mu_h)|$  in the second mesh refinement recommendation. In our computations in Section 12 we use the first mesh refinement recommendation and check the performance of this mesh refinement criterion.

**The first mesh refinement recommendation for IP.** Applying Theorem 5, we conclude that we should refine the mesh in neighborhoods of those points in  $\Omega_{\text{FEM}}$

where the function  $|h\varepsilon_h| + |h\mu_h|$  attains its maximal value. More precisely, we refine the mesh in such subdomains of  $\Omega_{\text{FEM}}$ , where

$$|h\varepsilon_h| + |h\mu_h| \geq \tilde{\beta} \max_{\Omega_{\text{FEM}}} (|h\varepsilon_h| + |h\mu_h|)$$

and where  $\tilde{\beta} \in (0, 1)$  is the number which should be chosen computationally and  $h$  is the mesh function (5.1) of the finite element mesh  $K_h$ .

**The second mesh refinement recommendation for IP.** Using Theorem 6, we conclude that we should refine the mesh in neighborhoods of those points in  $\Omega_{\text{FEM}}$ , where the function  $|J'_\varepsilon(\varepsilon_h, \mu_h)| + |J'_\mu(\varepsilon_h, \mu_h)|$  attains its maximal value. More precisely, let  $\beta \in (0, 1)$  be the tolerance number which should be chosen in computational experiments. Refine the mesh  $K_h$  in such subdomains of  $\Omega_{\text{FEM}}$ , where

$$|J'_\varepsilon(\varepsilon_h, \mu_h) + J'_\mu(\varepsilon_h, \mu_h)| \geq \beta \max_{\Omega_{\text{FEM}}} (|J'_\varepsilon(\varepsilon_h, \mu_h) + J'_\mu(\varepsilon_h, \mu_h)|).$$

**Remarks.** 1. We note that in (10.1), (10.2) we have exact values of  $E(x, t)$ ,  $\lambda(x, t)$  obtained with the computed functions  $(\varepsilon_h, \mu_h)$ . However, in our algorithms of Section 11 and in computations of Section 12 we approximate exact values of  $E(x, t)$ ,  $\lambda(x, t)$  by the computed ones  $E_h(x, t)$ ,  $\lambda_h(x, t)$ .

2. In both mesh refinement recommendations we used the fact that functions  $\varepsilon, \mu$  are unknown only in  $\Omega_{\text{FEM}}$ .

## 11. ALGORITHMS FOR THE SOLUTION OF IP

In this section we will present three different algorithms which can be used for the solution of our IP: the usual conjugate gradient algorithm and two different adaptive finite element algorithms. The conjugate gradient algorithm is applied on every finite element mesh  $K_h$  which we use in computations. We note that in our adaptive algorithms we refine not only the space mesh  $K_h$  but also the time mesh  $J_\tau$  accordingly to the CFL condition of [15]. However, the time mesh  $J_\tau$  is refined globally and not locally. It can be considered a new research task to check how the adaptive finite element method will work when both the space and time meshes are refined locally.

Taking into account the remark in Section 10, we denote

$$(11.1) \quad \begin{aligned} g_\varepsilon^n(x) = & - \int_0^T (\partial_t \lambda_h \partial_t E_h)(x, t, \varepsilon_h^n, \mu_h^n) dt + s \int_0^T (\nabla \cdot E_h)(\nabla \cdot \lambda_h)(x, t, \varepsilon_h^n, \mu_h^n) dt \\ & - \lambda_h(x, 0) f_1(x) + \gamma_1(\varepsilon_h^n - \varepsilon_0)(x), \quad x \in \Omega, \end{aligned}$$

(11.2)

$$g_\mu^n(x) = - \int_0^T ((\mu_h^n)^{-2} \nabla \times E_h \nabla \times \lambda_h)(x, t, \varepsilon_h^n, \mu_h^n) dt + \gamma_2(\mu_h^n - \mu_0)(x), \quad x \in \Omega,$$

where the functions  $\lambda_h, E_h$  are approximated finite element solutions of the state and adjoint problems computed with  $\varepsilon := \varepsilon_h^n$  and  $\mu := \mu_h^n$ , respectively, and  $n$  is the number of iterations in the conjugate gradient algorithm.

### 11.1. Conjugate Gradient Algorithm.

- Step 0.* Discretize the computational space-time domain  $\Omega \times [0, T]$  using partitions  $K_h$  and  $J_\tau$ , respectively, see Section 5. Start with the initial approximations  $\varepsilon_h^0 = \varepsilon_0$  and  $\mu_h^0 = \mu_0$  and compute the sequences of  $\varepsilon_h^n, \mu_h^n$ :
- Step 1.* Compute solutions  $E_h(x, t, \varepsilon_h^n, \mu_h^n)$  and  $\lambda_h(x, t, \varepsilon_h^n, \mu_h^n)$  of state (3.1) and adjoint (4.10) problems, respectively, using explicit schemes (5.13).
- Step 2.* Update the coefficients  $\varepsilon_h := \varepsilon_h^{n+1}$  and  $\mu_h := \mu_h^{n+1}$  on  $K_h$  and  $J_\tau$  via the conjugate gradient method:

$$\begin{aligned} \varepsilon_h^{n+1} &= \varepsilon_h^n + \alpha_\varepsilon d_\varepsilon^n(x), \\ \mu_h^{n+1} &= \mu_h^n + \alpha_\mu d_\mu^n(x), \end{aligned}$$

where

$$\begin{aligned} d_\varepsilon^n(x) &= -g_\varepsilon^n(x) + \beta_\varepsilon^n d_\varepsilon^{n-1}(x), \\ d_\mu^n(x) &= -g_\mu^n(x) + \beta_\mu^n d_\mu^{n-1}(x), \end{aligned}$$

with

$$\begin{aligned} \beta_\varepsilon^n &= \frac{\|g_\varepsilon^n(x)\|^2}{\|g_\varepsilon^{n-1}(x)\|^2}, \\ \beta_\mu^n &= \frac{\|g_\mu^n(x)\|^2}{\|g_\mu^{n-1}(x)\|^2}. \end{aligned}$$

Here,  $d_\varepsilon^0(x) = -g_\varepsilon^0(x), d_\mu^0(x) = -g_\mu^0(x)$  and  $\alpha_\varepsilon, \alpha_\mu$  are step-sizes in the gradient update which can be computed as in [28].

- Step 3.* Stop computing  $\varepsilon_h^n$  at the iteration  $M := n$  and obtain the function  $\varepsilon_h^M := \varepsilon_h^n$  if either  $\|g_1^n\|_{L^2(\Omega)} \leq \theta$  or the norms  $\|\varepsilon_h^n\|_{L^2(\Omega)}$  are stabilized. Here,  $\theta$  is the tolerance in  $n$  updates of the gradient method.
- Step 4.* Stop computing  $\mu_h^n$  at the iteration  $N := n$  and obtain the function  $\mu_h^N := \mu_h^n$  if either  $\|g_2^n\|_{L^2(\Omega)} \leq \theta$  or the norms  $\|\mu_h^n\|_{L^2(\Omega)}$  are stabilized. Otherwise set  $n := n + 1$  and go to step 1.

**11.2. Adaptive algorithms.** In this subsection we present two adaptive algorithms for the solution of our IP. In Adaptive algorithm 1 we apply the first mesh

refinement recommendation of Section 10, while in Adaptive algorithm 2 we use the second mesh refinement recommendation of Section 10.

We define the minimizer of the Tikhonov functional (4.1) and its approximated finite element solution on  $k$  times adaptively refined mesh  $K_{h_k}$  by  $(\varepsilon, \mu)$  and  $(\varepsilon_k, \mu_k)$ , correspondingly. In both our mesh refinement recommendations of Section 10 we need to compute the functions  $\varepsilon_k, \mu_k$  on the mesh  $K_{h_k}$ . To do that we apply the conjugate gradient algorithm of Section 11.1. We will define by  $\varepsilon_k := \varepsilon_h^M, \mu_k := \mu_h^N$  the values the obtained at steps 3 and 4 of the conjugate gradient algorithm.

### Adaptive Algorithm 1

*Step 0.* Choose an initial space-time mesh  $K_{h_0} \times J_{\tau_0}$  in  $\Omega_{\text{FEM}} \times [0, T]$ . Compute the sequences of  $\varepsilon_k, \mu_k, k > 0$ , via the following steps:

*Step 1.* Obtain numerical solutions  $\varepsilon_k, \mu_k$  on  $K_{h_k}$  using the Conjugate Gradient Method of Section 11.1.

*Step 2.* Refine such elements in the mesh  $K_{h_k}$ , where the inequality

$$(11.3) \quad |h\varepsilon_k| + |h\mu_k| \geq \tilde{\beta}_k \max_{\Omega_{\text{FEM}}} (|h\varepsilon_k| + |h\mu_k|)$$

is satisfied. Here, the tolerance numbers  $\tilde{\beta}_k \in (0, 1)$  are chosen by the user.

*Step 3.* Define a new refined mesh  $K_{h_{k+1}}$  and construct a new time partition  $J_{\tau_{k+1}}$  such that the CFL condition of [15] for explicit schemes (5.13) is satisfied. Interpolate  $\varepsilon_k, \mu_k$  on a new mesh  $K_{h_{k+1}}$  and perform steps 1–3 on the space-time mesh  $K_{h_{k+1}} \times J_{\tau_{k+1}}$ . Stop mesh refinements when  $\|\varepsilon_k - \varepsilon_{k-1}\| < \text{tol}_1$  and  $\|\mu_k - \mu_{k-1}\| < \text{tol}_2$  or  $\|g_\varepsilon^k(x)\| < \text{tol}_3$  and  $\|g_\mu^k(x)\| < \text{tol}_4$ , where  $\text{tol}_i, i = 1, \dots, 4$  are tolerances chosen by the user.

### Adaptive Algorithm 2

*Step 0.* Choose an initial space-time mesh  $K_{h_0} \times J_{\tau_0}$  in  $\Omega_{\text{FEM}}$ . Compute the sequence  $\varepsilon_k, \mu_k, k > 0$ , on a refined meshes  $K_{h_k}$  via the following steps:

*Step 1.* Obtain numerical solutions  $\varepsilon_k, \mu_k$  on  $K_{h_k} \times J_{\tau_k}$  using the Conjugate Gradient Method of Section 11.1.

*Step 2.* Refine the mesh  $K_{h_k}$  at all points, where

$$(11.4) \quad |g_\varepsilon^k(x)| + |g_\mu^k(x)| \geq \beta_k \max_{\Omega} (|g_\varepsilon^k(x)| + |g_\mu^k(x)|),$$

and where a posteriori error indicators  $g_\varepsilon^k, g_\mu^k$  are defined in (10.1), (11.1). We choose the tolerance number  $\beta_k \in (0, 1)$  in numerical examples.

*Step 3.* Define a new refined mesh  $K_{h_{k+1}}$  and construct a new time partition  $J_{\tau_{k+1}}$  such that the CFL condition of [15] for explicit schemes (5.13) is satisfied.

Interpolate  $\varepsilon_k, \mu_k$  on a new mesh  $K_{h_{k+1}}$  and perform steps 1–3 on the space-time mesh  $K_{h_{k+1}} \times J_{\tau_{k+1}}$ . Stop mesh refinements when  $\|\varepsilon_k - \varepsilon_{k-1}\| < \text{tol}_1$  and  $\|\mu_k - \mu_{k-1}\| < \text{tol}_2$  or  $\|g_\varepsilon^k(x)\| < \text{tol}_3$  and  $\|g_\mu^k(x)\| < \text{tol}_4$ , where  $\text{tol}_i, i = 1, \dots, 4$ , are tolerances chosen by the user.

**Remarks.** 1. First we make comments how to choose the tolerance numbers  $\beta_k, \widetilde{\beta}_k$  in (11.4), (11.3). Their values depend on the concrete values of  $\max_{\Omega_{\text{FEM}}} (|g_\varepsilon^k(x)| + |g_\mu^k(x)|)$  and  $\max_{\Omega_{\text{FEM}}} (|h\varepsilon_k| + |h\mu_k|)$ , correspondingly. If we take values of  $\beta_k, \widetilde{\beta}_k$  which are very close to 1 then we refine the mesh in a very narrow region of the  $\Omega_{\text{FEM}}$ , and if we choose  $\beta_k, \widetilde{\beta}_k \approx 0$  then almost all elements in the finite element mesh will be refined, and thus, we will get a global and not local mesh refinement. Our numerical tests in Section 12 show that the choice of  $\beta_k, \widetilde{\beta}_k = 0.7$  is almost optimal one since with these values of the parameters  $\beta_k, \widetilde{\beta}_k$  the finite element mesh  $K_h$  is refined exactly at the places where we have computed the functions  $(\varepsilon_h, \mu_h)$ .

2. To compute  $L^2$ -norms  $\|\varepsilon_k - \varepsilon_{k-1}\|, \|\mu_k - \mu_{k-1}\|$  in step 3 of the adaptive algorithms the solutions  $\varepsilon_{k-1}, \mu_{k-1}$  are interpolated from the mesh  $K_{h_{k-1}}$  to the mesh  $K_{h_k}$ .

## 12. NUMERICAL STUDIES OF THE ADAPTIVITY TECHNIQUE

In this section we present numerical tests for the solution of our IP using the adaptive algorithm 1 of Section 11.2. The goal of our simulations is to show the performance of the adaptivity technique in order to improve the reconstruction which was obtained on a coarse non-refined mesh.

In our tests we reconstruct two symmetric structures of Figure 1 which represent the model of a waveguide with small magnetic metallic inclusions with the relative permittivity  $\varepsilon = 12$  and the relative magnetic permeability  $\mu = 2.0$ . We note that we choose  $\varepsilon = 12$  in metallic targets similarly to our recent work [6] and experimental work [10], where metallic targets were treated as dielectrics with large dielectric constants and were called *effective* dielectric constants. Their values were chosen similarly to [6] and [10] in the interval

$$(12.1) \quad \varepsilon \in (10, 30).$$

In our tests we choose  $\mu = 2.0$ , because the relative magnetic permeability belongs to the interval  $\mu \in [1, 3]$ , see [30] and [6] for a similar choice.

As in [6] we initialize only one component  $E_2$  of the electrical field  $E = (E_1, E_2, E_3)$  on  $S_T$  as a plane wave  $f(t)$  such that (see boundary condition in (3.1))

$$(12.2) \quad f(t) = \begin{cases} \sin(\omega t) & \text{if } t \in \left(0, \frac{2\pi}{\omega}\right), \\ 0 & \text{if } t > \frac{2\pi}{\omega}. \end{cases}$$

Compared with [6], where in computations only zero initial conditions were used in (3.1), in Test 2 of our study we use a non-zero initial condition for the second component  $E_2$  given by the function

$$(12.3) \quad \begin{aligned} f_0(x) &= E_2(x, 0) = e^{-(x_1^2 + x_2^2 + x_3^3)} \cdot \cos t \Big|_{t=0} = e^{-(x_1^2 + x_2^2 + x_3^3)}, \\ f_1(x) &= \frac{\partial E_2}{\partial t}(x, 0) = -e^{-(x_1^2 + x_2^2 + x_3^3)} \cdot \sin t \Big|_{t=0} \equiv 0. \end{aligned}$$

We perform two different tests with different inclusions to be reconstructed:

*Test 1.* Reconstruction of two layers of scatterers of Figure 1b) with additive noise  $\sigma = 7\%$  and  $\sigma = 17\%$  in backscattered data on the frequency interval  $\omega \in [45, 60]$  with zero initial conditions in (3.1).

*Test 2.* Reconstruction of one layer of scatterers of Figure 1d) with additive noise  $\sigma = 7\%$  and  $\sigma = 17\%$  in backscattered data on the frequency interval  $\omega \in [45, 60]$  with one non-zero initial condition (12.3) in (3.1).

**12.1. Computational domains.** For simulations of forward and adjoint problems we use the domain decomposition method of [5]. This method is convenient for our computations, since it is efficiently implemented in the software package WavES [33] using PETSc [27]. To apply the method of [5] we divide our computational domain  $\Omega$  into two subregions as described in Section 3, and define  $\Omega_{\text{FDM}} := \Omega_{\text{OUT}}$  such that  $\overline{\Omega} = \overline{\Omega}_{\text{FEM}} \cup \overline{\Omega}_{\text{FDM}}$ , see Figure 1. In  $\Omega_{\text{FEM}}$  we use finite elements and in  $\Omega_{\text{FDM}}$  we use the finite difference method. We set functions  $\varepsilon(x) = \mu(x) = 1$  in  $\Omega_{\text{FDM}}$  and assume that they are unknown only in  $\Omega_{\text{FEM}}$ . We choose the dimensionless domain  $\Omega_{\text{FEM}}$  such that

$$\Omega_{\text{FEM}} = \{x' = (x_1, x_2, x_3) \in (-3.2, 3.2) \times (-0.6, 0.6) \times (-0.6, 0.6)\}$$

and the dimensionless domain  $\Omega$  is set to be

$$\Omega = \{x' = (x_1, x_2, x_3) \in (-3.4, 3.4) \times (-0.8, 0.8) \times (-0.8, 0.8)\}.$$

Here, the dimensionless spatial variable is  $x' = x/1$  m. In the domain decomposition between  $\Omega_{\text{FEM}}$  and  $\Omega_{\text{FDM}}$  we choose the mesh size  $h = 0.1$ . We use also this mesh

size for the coarse mesh  $K_{h_0}$  in both adaptive algorithms of Section 11.2. As in [5], [4], [6] in all our tests we set  $s = 1$  in (3.1) in  $\Omega_{\text{FEM}}$ .

Because of the domain decomposition Maxwell's system (3.1) transforms to the wave equation in  $\Omega_{\text{FDM}}$  and in  $\Omega_{\text{FEM}}$  and we solve Maxwell's system (3.1) with boundary conditions obtained from the finite difference method; these systems for the forward and adjoint problems are presented in [6]. We solve the forward and adjoint problems in time  $[0, T] = [0, 3]$  by both adaptive algorithms and choose the time step  $\tau = 0.006$  which satisfies the CFL condition [15]. To be able to test adaptive algorithms we first generate backscattered data at  $S_T$  by solving the forward problem (3.1) with the plane wave  $f(t)$  given by (12.2) in the time interval  $t = [0, 3]$  with  $\tau = 0.006$  and with known values of  $\varepsilon_r = 12.0$ ,  $\mu = 2$  inside the scatterers of Figure 1 and  $\varepsilon = \mu = 1.0$  everywhere else in  $\Omega$ . Our data were generated on a specially constructed mesh for the solution of the forward problem: this mesh was several times refined in the places where inclusions of Figure 1 are located. This mesh is completely different from the meshes used in computations in Tests 1, 2. Thus, the variational crime in our computations is avoided.

**12.2. Reconstructions.** We start to run adaptive algorithms with guess values of  $\varepsilon = 1.0$ ,  $\mu = 1.0$  at all points in  $\Omega$ . In our recent work [6] it was shown that such choice of the initial guess gives a good reconstruction for both functions  $\varepsilon$  and  $\mu$ , see also [2], [5] for a similar choice of initial guess for other coefficient inverse problems (CIPs). Taking into account (12.1), we choose the following sets of admissible parameters for  $\varepsilon$  and  $\mu$ :

$$(12.4) \quad \begin{aligned} M_\varepsilon &\in \{\varepsilon \in C(\overline{\Omega}) \mid 1 \leq \varepsilon(x) \leq 15\}, \\ M_\mu &\in \{\mu \in C(\overline{\Omega}) \mid 1 \leq \mu(x) \leq 3\}. \end{aligned}$$

In our simulations we choose two constant regularization parameters  $\gamma_1 = 0.01$ ,  $\gamma_2 = 0.7$  in the Tikhonov functional (4.1). These parameters satisfy conditions (6.8) and were chosen because of our computational experience: such choices for the regularization parameters were optimal since they gave the smallest relative errors  $e_\varepsilon = \|\varepsilon - \varepsilon_h\|/\|\varepsilon_h\|$  and  $e_\mu = \|\mu - \mu_h\|/\|\mu_h\|$  in the reconstruction, see [6] for details. Iteratively regularized adaptive finite element method for our IP when zero initial conditions  $f_0 = f_1 = 0$  in (3.1) are initialized, was recently presented in [18]. Currently we perform numerical experiments with iteratively regularized adaptive finite element method for the case when we initialize one non-zero initial condition (12.3) in (3.1). This work will be described in the forthcoming paper. In the above mentioned works iterative regularization is performed via algorithms of [2]. We also refer to [16], [19] for different techniques for the choice of regularization parameters.

To get our reconstructions of Figures 2–4, we use the image post-processing procedure described in [6]. Tables 1–4 present computed results of reconstructions for  $\varepsilon$  and  $\mu$  on different adaptively refined meshes after applying adaptive algorithm 1. Similar results are obtained for adaptive algorithm 2, and thus they are not presented here.

$\sigma = 7\%$						
Test 1	$\max_{\Omega_{\text{FEM}}} \varepsilon_{\overline{N}}$	error, %	$\overline{N}$	$\max_{\Omega_{\text{FEM}}} \mu_{\overline{M}}$	error, %	$\overline{M}$
$\omega = 45$	14.96	24.6	3	1.82	9	3
$\omega = 50$	14.96	24.6	3	1.73	13.5	3
$\omega = 60$	14.95	24.5	3	1.76	12	3
Test 2	$\max_{\Omega_{\text{FEM}}} \varepsilon_{\overline{N}}$	error, %	$\overline{N}$	$\max_{\Omega_{\text{FEM}}} \mu_{\overline{M}}$	error, %	$\overline{M}$
$\omega = 45$	12.97	8	3	1.99	0.5	3
$\omega = 50$	14.57	21.4	3	1.79	10.5	3
$\omega = 60$	9.3	22.5	3	1.91	4.5	3

Table 1. Results of reconstruction on a 5 times adaptively refined meshes of Tables 3, 4 for  $\sigma = 7\%$  together with computational errors between  $\max_{\Omega_{\text{FEM}}} \varepsilon_{\overline{N}}$  and exact  $\varepsilon^*$  in percents. Here,  $\overline{N}$  is the final iteration number in the conjugate gradient method for computation of  $\varepsilon$ , and  $\overline{M}$  is the final iteration number for computation of  $\mu$ .

$\sigma = 17\%$						
Test 1	$\max_{\Omega_{\text{FEM}}} \varepsilon_{\overline{N}}$	error, %	$\overline{N}$	$\max_{\Omega_{\text{FEM}}} \mu_{\overline{M}}$	error, %	$\overline{M}$
$\omega = 45$	14.96	24.6	3	1.65	17.5	3
$\omega = 50$	14.96	24.6	3	1.97	1.5	3
$\omega = 60$	14.95	24.5	3	2.04	20	3
Test 2	$\max_{\Omega_{\text{FEM}}} \varepsilon_{\overline{N}}$	error, %	$\overline{N}$	$\max_{\Omega_{\text{FEM}}} \mu_{\overline{M}}$	error, %	$\overline{M}$
$\omega = 45$	14.69	22.4	3	1.71	14.5	3
$\omega = 50$	14.47	20.5	3	1.63	18.5	3
$\omega = 60$	8.44	29.7	3	1.74	13	3

Table 2. Results of reconstruction on a 5 times adaptively refined meshes of Tables 3 and 4 for  $\sigma = 17\%$  together with computational errors between  $\max_{\Omega_{\text{FEM}}} \varepsilon_{\overline{N}}$  and exact  $\varepsilon^*$  in percents. Here,  $\overline{N}$  is the final iteration number in the conjugate gradient method for computation of  $\varepsilon$ , and  $\overline{M}$  is the final iteration number for computation of  $\mu$ .

To get our reconstructions of Figures 2–4, we use the image post-processing procedure described in [6]. Tables 1–4 present computed results of reconstructions for  $\varepsilon$  and  $\mu$  on different adaptively refined meshes after applying adaptive algorithm 1.

$\omega$	coarse mesh	1 ref. mesh	2 ref. mesh	3 ref. mesh	4 ref. mesh	5 ref. mesh
45 # nodes	10958	11028	11241	11939	14123	18750
# elements	55296	55554	56624	60396	73010	96934
$\varepsilon_r^{\text{comp}}$	15	15	15	15	15	14.96
$\mu_r^{\text{comp}}$	2.58	2.58	2.58	2.58	2.58	1.82
50 # nodes	10958	11031	11212	11887	13761	17892
# elements	55296	55572	56462	60146	71010	92056
$\varepsilon_r^{\text{comp}}$	15	15	15	15	15	14.96
$\mu_r^{\text{comp}}$	2.38	2.38	2.38	2.38	2.38	1.73
60 # nodes	10958	11050	11255	11963	13904	18079
# elements	55296	56666	60564	71892	61794	92926
$\varepsilon_r^{\text{comp}}$	15	15	15	15	15	14.96
$\mu_r^{\text{comp}}$	2.46	2.46	2.46	2.46	2.46	1.76

Table 3. Test 1. Computed values of  $\varepsilon_r^{\text{comp}} := \max_{\Omega_{\text{FEM}}} \varepsilon$  and  $\mu_r^{\text{comp}} := \max_{\Omega_{\text{FEM}}} \mu$  on the adaptively refined meshes. Computations are done with the noise  $\sigma = 7\%$ .

$\omega$	coarse mesh	1 ref. mesh	2 ref. mesh	3 ref. mesh	4 ref. mesh	5 ref. mesh
45 # nodes	10958	11007	11129	11598	12468	14614
# elements	55428	55428	56024	58628	63708	74558
$\varepsilon_r^{\text{comp}}$	15	15	15	15	15	14.96
$\mu_r^{\text{comp}}$	2.39	2.39	2.39	2.39	2.39	1.71
50 # nodes	10958	11002	11106	11527	12433	14494
# elements	55296	55398	55908	58240	63540	73900
$\varepsilon_r^{\text{comp}}$	15	15	15	15	15	14.47
$\mu_r^{\text{comp}}$	2.24	2.24	2.24	2.24	2.24	1.63
60 # nodes	10958	11002	11104	11560	12459	14888
# elements	55296	55398	55904	58402	63628	76068
$\varepsilon_r^{\text{comp}}$	8.46	8.46	8.46	8.46	8.46	8.44
$\mu_r^{\text{comp}}$	2.50	2.50	2.50	2.50	2.50	1.74

Table 4. Test 2. Computed values of  $\varepsilon_r^{\text{comp}} := \max_{\Omega_{\text{FEM}}} \varepsilon$  and  $\mu_r^{\text{comp}} := \max_{\Omega_{\text{FEM}}} \mu$  on the adaptively refined meshes. Computations are done with the noise  $\sigma = 17\%$ .

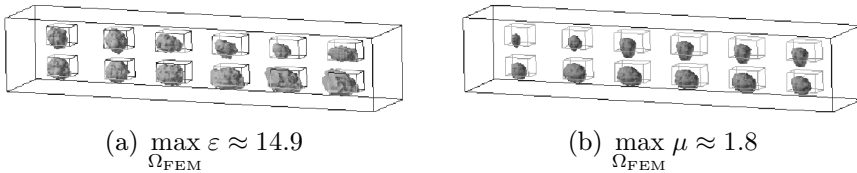


Figure 2. Test 1. Computed images of reconstructed functions  $\varepsilon(\mathbf{x})$  and  $\mu(\mathbf{x})$  on a 5 times adaptively refined mesh. Computations are done for  $\omega = 45$ ,  $\sigma = 7\%$ .

Similar results are obtained for adaptive algorithm 2, and thus they are not presented here.

**12.2.1. Test 1.** In this example we performed simulations with two additive noise levels in the data:  $\sigma = 7\%$  and  $\sigma = 17\%$ , see Tables 1–4 for results. Using these tables, we observe that the best reconstruction results for both the noise levels are obtained for  $\omega = 45$  in (12.2). Below we describe the reconstructions for  $\omega = 45$  in (12.2) and  $\sigma = 7\%$ .

We achieve good values of contrast for both functions already on a coarse mesh, see Tables 1, 2 of [7]. However, Figures 3a), b) show us that the locations of all inclusions in  $x_3$  direction should be improved. The reconstructions of  $\varepsilon$  and  $\mu$  on the final adaptively refined mesh are presented in Figure 2. We observe significant improvement of reconstructions of  $\varepsilon$  and  $\mu$  in  $x_3$  direction on the final adaptively refined mesh compared with reconstructions obtained on the coarse mesh, see Figure 3.

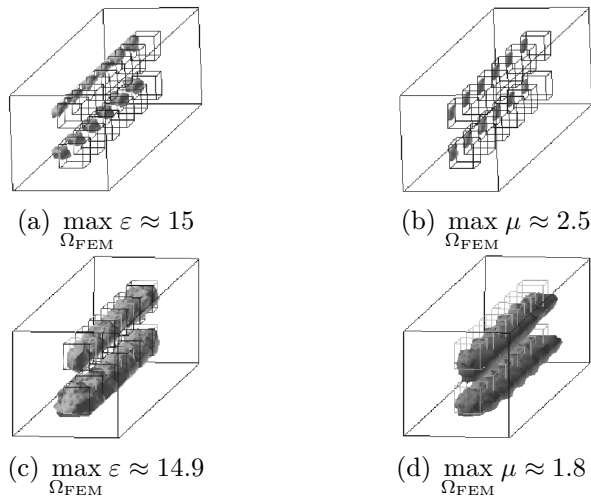


Figure 3. Test 1. Computed images of reconstructed functions  $\varepsilon(\mathbf{x})$  and  $\mu(\mathbf{x})$  in  $x_2x_3$  view: a), b) on a coarse mesh, c), d) on a 5 times adaptively refined mesh. Computations are done for  $\omega = 45$ ,  $\sigma = 7\%$ .

**12.2.2. Test 2.** In this test we again used two additive noise levels in the data,  $\sigma = 7\%$  and  $\sigma = 17\%$ , as well as the non-zero initial condition (12.3) in (3.1). Results of computations are presented in Tables 1–4. Using these tables, we see that the best reconstruction results in this test for both the noise levels are obtained for  $\omega = 50$  in (12.2). The reconstructions of  $\varepsilon$  and  $\mu$  on the final adaptively refined mesh for  $\omega = 50$  in (12.2) and  $\sigma = 17\%$  are given in Figure 4. We again observe significant improvement of reconstructions of  $\varepsilon$  and  $\mu$  in  $x_3$  direction on the final adaptively refined mesh in comparison to the reconstruction obtained on the coarse mesh, see Figure 5.

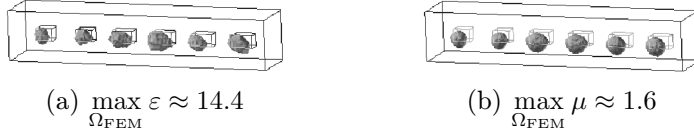


Figure 4. Test 2. Computed images of reconstructed functions  $\varepsilon(\mathbf{x})$  and  $\mu(\mathbf{x})$  on a 5 times adaptively refined mesh. Computations are done with  $\omega = 50$ ,  $\sigma = 17\%$ .

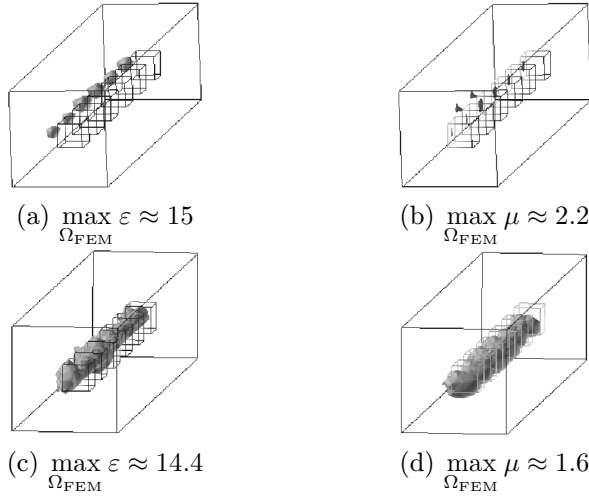


Figure 5. Test 2. Computed images of reconstructed functions  $\varepsilon(\mathbf{x})$  and  $\mu(\mathbf{x})$  in  $x_2x_3$  view: a), b) on a coarse mesh, c), d) on a 5 times adaptively refined mesh. Computations are done for  $\omega = 50$ ,  $\sigma = 17\%$ .

### 13. CONCLUSION

In this work we derived a posteriori error estimates in the reconstructed coefficients  $\varepsilon$  and  $\mu$  and in the Tikhonov functional to be minimized. Numerically we tested our algorithms with two different noise levels,  $\sigma = 7\%$  and  $\sigma = 17\%$ , on the frequency band  $\omega \in [45, 60]$ . The main conclusion of our previous study [6] was that we could get large contrast of the dielectric function  $\varepsilon$  which allows us to reconstruct metallic targets, and that the contrast for  $\mu$  was within limits of (12.4). However, the size of  $\mu$  in  $x_1, x_2$  directions and the location of all inclusions in  $x_3$  direction should be improved. We get results similar to those obtained in [6] on a coarse mesh. However, with mesh refinements, as was expected, the quality of reconstruction improved a lot, see Figures 3, 4, 5. Using these Figures and Tables 1–4 we observe that now all inclusions have correct locations in  $x_3$  direction and their contrasts and sizes in  $x_1, x_2$  directions are also improved and reconstructed with a good accuracy. We can conclude that we have supported tests of our previous works [3], [4], [10], [9], [21]

and have shown that the adaptive finite element method is a powerful tool for the reconstruction of coefficients in Maxwell's equations from limited observations.

#### References

- [1] *F. Assous, P. Degond, E. Heintze, P. A. Raviart, J. Segre*: On a finite-element method for solving the three-dimensional Maxwell equations. *J. Comput. Phys.* *109* (1993), 222–237.
- [2] *A. B. Bakushinsky, M. Y. Kokurin, A. Smirnova*: Iterative Methods for Ill-Posed Problems. An Introduction. Inverse and Ill-Posed Problems Series 54, Walter de Gruyter, Berlin, 2011.
- [3] *L. Beilina*: Adaptive hybrid FEM/FDM methods for inverse scattering problems. *Inverse Problems and Information Technologies*, V.1, N.3 (2002), 73–116.
- [4] *L. Beilina*: Adaptive finite element method for a coefficient inverse problem for Maxwell's system. *Appl. Anal.* *90* (2011), 1461–1479.
- [5] *L. Beilina*: Energy estimates and numerical verification of the stabilized domain decomposition finite element/finite difference approach for time-dependent Maxwell's system. *Cent. European J. Math.* *11* (2013), 702–733, DOI 10.2478/s11533-013-0202-3.
- [6] *L. Beilina, M. Cristofol, K. Niinimäki*: Optimization approach for the simultaneous reconstruction of the dielectric permittivity and magnetic permeability functions from limited observations. *Inverse Probl. Imaging* *9* (2015), 1–25.
- [7] *L. Beilina, S. Hosseinzadegan*: An adaptive finite element method in reconstruction of coefficients in Maxwell's equations from limited observations. ArXiv:1510.07525 (2015).
- [8] *L. Beilina, M. V. Klibanov*: Approximate Global Convergence and Adaptivity for Coefficient Inverse Problems. Springer, New York, 2012.
- [9] *L. Beilina, M. V. Klibanov, M. Yu. Kokurin*: Adaptivity with relaxation for ill-posed problems and global convergence for a coefficient inverse problem. *J. Math. Sci., New York* *167* (2010), 279–325; translation from *Probl. Mat. Anal.* *46* (2010), 3–44. (In Russian original.)
- [10] *L. Beilina, N. T. Thành, M. V. Klibanov, J. B. Malmberg*: Reconstruction of shapes and refractive indices from backscattering experimental data using the adaptivity. *Inverse Probl.* *30* (2014), 28 pages, Article ID 105007.
- [11] *M. Bellassoued, M. Cristofol, E. Soccorsi*: Inverse boundary value problem for the dynamical heterogeneous Maxwell's system. *Inverse Probl.* *28* (2012), 18 pages, Article ID 095009.
- [12] *S. C. Brenner, L. R. Scott*: The Mathematical Theory of Finite Element Methods. Texts in Applied Mathematics 15, Springer, Berlin, 2002.
- [13] *P. Ciarlet, Jr., H. Wu, J. Zou*: Edge element methods for Maxwell's equations with strong convergence for Gauss' laws. *SIAM J. Numer. Anal.* *52* (2014), 779–807.
- [14] *G. C. Cohen*: Higher Order Numerical Methods for Transient Wave Equations. Scientific Computation, Springer, Berlin, 2002.
- [15] *R. Courant, K. Friedrichs, H. Lewy*: On the partial difference equations of mathematical physics. *IBM J. Res. Dev.* *11* (1967), 215–234.
- [16] *H. W. Engl, M. Hanke, A. Neubauer*: Regularization of Inverse Problems. Mathematics and Its Applications 375, Kluwer Academic Publishers, Dordrecht, 1996.
- [17] *K. Eriksson, D. Estep, C. Johnson*: Applied Mathematics: Body and Soul. Vol. 3. Calculus in Several Dimensions. Springer, Berlin, 2004.
- [18] *S. Hosseinzadegan*: Iteratively regularized adaptive finite element method for reconstruction of coefficients in Maxwell's system. Master's Thesis in Applied Mathematics, Department of Mathematical Sciences, Chalmers University of Technology and Gothenburg University, 2015.

- [19] *K. Ito, B. Jin, T. Takeuchi*: Multi-parameter Tikhonov regularization. *Methods Appl. Anal.* 18 (2011), 31–46.
- [20] *C. Johnson, A. Szepessy*: Adaptive finite element methods for conservation laws based on a posteriori error estimates. *Commun. Pure Appl. Math.* 48 (1995), 199–234.
- [21] *M. V. Klibanov, A. B. Bakushinsky, L. Beilina*: Why a minimizer of the Tikhonov functional is closer to the exact solution than the first guess. *J. Inverse Ill-Posed Probl.* 19 (2011), 83–105.
- [22] *M. Křížek, P. Neittaanmäki*: Finite Element Approximation of Variational Problems and Applications. Pitman Monographs and Surveys in Pure and Applied Mathematics 50, Longman Scientific & Technical, Harlow; John Wiley & Sons, New York, 1990.
- [23] *O. A. Ladyzhenskaya*: The Boundary Value Problems of Mathematical Physics. Springer, New York, 1985.
- [24] *J. B. Malmberg*: A posteriori error estimation in a finite element method for reconstruction of dielectric permittivity. ArXiv:1502.07658 (2015).
- [25] *J. B. Malmberg*: A posteriori error estimate in the Lagrangian setting for an inverse problem based on a new formulation of Maxwell’s system. Inverse Problems and Applications (L. Beilina, ed.). Selected Papers Based on the Presentations at the Third Annual Workshop on Inverse Problems, Stockholm, 2013, Springer Proceedings in Mathematics and Statistics 120, 2015, pp. 43–53.
- [26] *C. D. Munz, P. Omnes, R. Schneider, E. Sonnendrücker, U. Voß*: Divergence correction techniques for Maxwell solvers based on a hyperbolic model. *J. Comput. Phys.* 161 (2000), 484–511.
- [27] PETSc, Portable, Extensible Toolkit for Scientific Computation. <http://www.mcs.anl.gov/petsc/>.
- [28] *O. Pironneau*: Optimal Shape Design for Elliptic Systems. Springer Series in Computational Physics, Springer, New York, 1984.
- [29] *L. R. Scott, S. Zhang*: Finite element interpolation of nonsmooth functions satisfying boundary conditions. *Math. Comput.* 54 (1990), 483–493.
- [30] *D. R. Smith, S. Schultz, P. Markoš, C. M. Soukoulis*: Determination of effective permittivity and permeability of metamaterials from reflection and transmission coefficients. *Phys. Rev. B* 65 (2002), DOI:10.1103/PhysRevB.65.195104.
- [31] *A. N. Tikhonov, A. V. Goncharskiy, V. V. Stepanov, I. V. Kochikov*: Ill-posed problems of the image processing. *DAN USSR* 294 (1987), 832–837.
- [32] *A. N. Tikhonov, A. V. Goncharsky, V. V. Stepanov, A. G. Yagola*: Numerical Methods for the Solution of Ill-Posed Problems. *Rev. Mathematics and Its Applications* 328, Kluwer Academic Publishers, Dordrecht, 1995.
- [33] WavES: The software package. <http://www.waves24.com>.

*Authors’ addresses:* Larisa Beilina, Department of Mathematical Sciences, Chalmers University of Technology and Gothenburg University, SE-42196 Göteborg, Sweden, e-mail: [larisa@chalmers.se](mailto:larisa@chalmers.se); Samar Hosseinzadegan, Department of Signals and Systems, Chalmers University of Technology, SE-42196 Göteborg, Sweden, e-mail: [samarh@chalmers.se](mailto:samarh@chalmers.se).